“Basic research is when I am doing what I don't know what I am doing.”
Wernher von Braun (1912-1977)

University of Alberta

HSV-1 VP11/12-mediated initiation of
Src family kinase-PI3 kinase-Akt signalling

by

Frederick W. Wu

A thesis submitted to the Faculty of Graduate Studies and Research
in partial fulfillment of the requirements for the degree of

Master of Science
in
Virology

Department of Medical Microbiology and Immunology

Fall 2013
Edmonton, Alberta

To Ellen and Charles, my parents,

who, like many parents, tried hard to screw up their children,

who, unlike many parents, failed to do so,

to whom I am grateful for this glorious and fortunate failure

To Margaret, my sister,

who is awesome,

who embodies awesomeness,

from whom I am learning what awesomeness is

Abstract

Herpes simplex virus type 1 is a ubiquitous human virus that causes cold sores and, increasingly, genital herpes. Upon virion-cell fusion, tegument proteins diffuse into host cytosol and, as such, are poised to remodel signalling pathways. Tegument proteins of interest here are virion protein 11/12 (VP11/12) and US3 protein kinase (US3PK), for its potential role in VP11/12 regulation. Wagner and Smiley (2011) posited a model wherein VP11/12 commandeers Lck to activate Akt. This study tests this model using various *in vitro* assays to dissect VP11/12 interaction with the Lck SH2 domain. My findings support the Wagner-Smiley model. To address curiosities in prior US3PK characterization, I generated US3-null mutants from wild-type and UL46-null viruses to produce US3- and UL46-null single and double knock-outs derived from KOS-37. Preliminary analysis of US3 mutants shows US3PK-dependent VP11/12 modification. These mutants allow for further exploration of US3PK-VP11/12 interplay.

Acknowledgements

I am honoured to count Dr. Jim Smiley among a small handful of people who have profoundly influenced how I think and learn, and it was my privilege to have his mentorship over the course of this research. I am indebted to Dr. Melany Wagner, who originally discovered VP11/12-induced Akt activation, for the puzzles her work has illuminated for others to solve. Various members of the Smiley laboratory provided invaluable technical assistance and advice, in particular Holly Saffran and Dr. Bianca Dauber. The Smiley lab offered useful and insightful discussion drawn from a wide breadth of experience; I mention Brett Duguay and Dr. Heather Eaton for their consistent availability for discussion and input. Labmate Kevin Quach was a pleasure to work with and the consummate teammate. I thank Dr. Debby Burshtyn, department graduate coordinator, for support throughout my graduate program. I further thank Drs. Michele Barry and Rob Ingham, supervisory committee members, for holding me accountable to the standard this research deserves.

Table of Contents

List of Figures

List of Tables

List of Abbreviations

α	anti (unless a literal 'alpha')
2-ME	2-mercaptoethanol
4E-BP1	eukaryotic translation initiation factor 4E-binding protein
AMPK	5' adenosine monophosphate-activated protein kinase
ATCC	American Type Culture Collection
BAC	bacterial artificial chromosome
BAD	Bcl-2-associated death promoter
Bcl-2	B-cell lymphoma 2
Bid	Bcl-2 homology 3-interacting domain death agonist
bp	basepair(s)
BSA	bovine serum albumin
CD	cluster of differentiation
CDK	cyclin-dependent kinase
CMV	cytomegalovirus
diH2O	deionized water
DMEM	Dulbecco’s modified Eagle's medium
DNA	deoxyribonucleic acid
DOG	2-deoxygalactose
dsDNA	double-stranded DNA
EBV	Epstein-Barr virus
ECL	enhanced chemiluminescence

EDTA	ethylenediaminetetraacetic acid
ELM	eukaryotic linear motif
FBS	fetal bovine serum
FKBP38	FK506-binding protein 8
FOXO	forkhead box class O
gB	glycoprotein B
gC	glycoprotein C
gD	glycoprotein D
GFP	green fluorescent protein
gH	glycoprotein H
gL	glycoprotein L
GLAB	GST lysis and binding
Grb2	growth factor receptor-bound protein 2
GSK3	glycogen synthase kinase 3
GST	glutathione s-transferase
HDAC	histone deacetylase
HEL	human embryonic lung
HHV-6	*Human herpesvirus 6*
HHV-7	*Human herpesvirus 7*
hpi	hours post-infection
HRP	horseradish peroxidase
HSV-1	Herpes simplex virus type 1

HSV-2	Herpes simplex virus type 2
IE	immediate-early
IFN	interferon
IPTG	isopropyl β-D-1-thiogalactopyranoside
IR	infrared or insulin receptor
IRS-1	insulin receptor substrate 1
KSHV	Kaposi's sarcoma-associated herpesvirus
LAT	latency-associated transcript
LB	Luria-Burtani
MAFFT	Multiple Alignment using Fast Fourier Transform
mTag	middle T antigen
mTOR	mammalian target of rapamycin
mTORC	mTOR complex
MW	molecular weight
NS	viral nonstructural protein
OBB	Odyssey blocking buffer
Oct	octamer transcription factor
OD	optical density
ORF	open reading frame
p	phospho
PAGE	polyacrylamide gel electrophoresis
PBMC	peripheral blood mononuclear cell

PBS	phosphate-buffered saline
PCR	polymerase chain reaction
PD	pull-down
PDK	phosphoinositide-dependent protein kinase
PFU	plaque-forming units
PH	pleckstrin-homology
PI3K	phosphatidylinositol 3-kinase
PIP2	phosphatidylinositol 4,5-bisphosphate
PIP3	phosphatidylinositol 3,4,5-triphosphate
PSI-BLAST	position-specific iterative basic local alignment search tool
PTB	phosphotyrosine-binding (domain)
PTEN	phosphatase and tensin homolog (protein)
RPMI	Roswell Park Memorial Institute medium
rpS6	ribosomal protein S6
S6	ribosomal protein S6
S6K	S6 kinase
SA	streptavidin-agarose
SDS	sodium dodecylsulfate
SFK	Src-family kinase
SH	Src-homology
Shc	SH2 domain-containing (protein)
SOS	Son of Sevenless (protein)

spp.	species (plural)
STI	sexually transmitted infection
TAE	Tris-acetate-EDTA
TBS-T	Tris-buffered saline with Tween
Tris	tris(hydroxymethyl)aminomethane
TSC	tuberous sclerosis protein
U	units
UL	unique-long
US	unique-short
US3PK	unique-short 3 protein kinase
VP	virion protein
VP11/12	virion protein 11/12

Chapter I

Introduction

1.1 HERPES SIMPLEX VIRUS TYPE 1

1.1.1 Overview of herpesviruses

Herpesviruses are those viruses of the order *Herpesvirales* (Davison *et al*., 2009). These viruses were originally classified as herpesviruses based on a shared virion morphology, distinct from all other viruses (Pellett and Roizman, 2007). The virion is composed of a double-stranded DNA genome contained within an icosahedral capsid, surrounded by a proteinaceous layer called the tegument, all enveloped by a lipid membrane with glycoprotein spikes (Figure 1-1). Each virion has a diameter of about 120 nm.

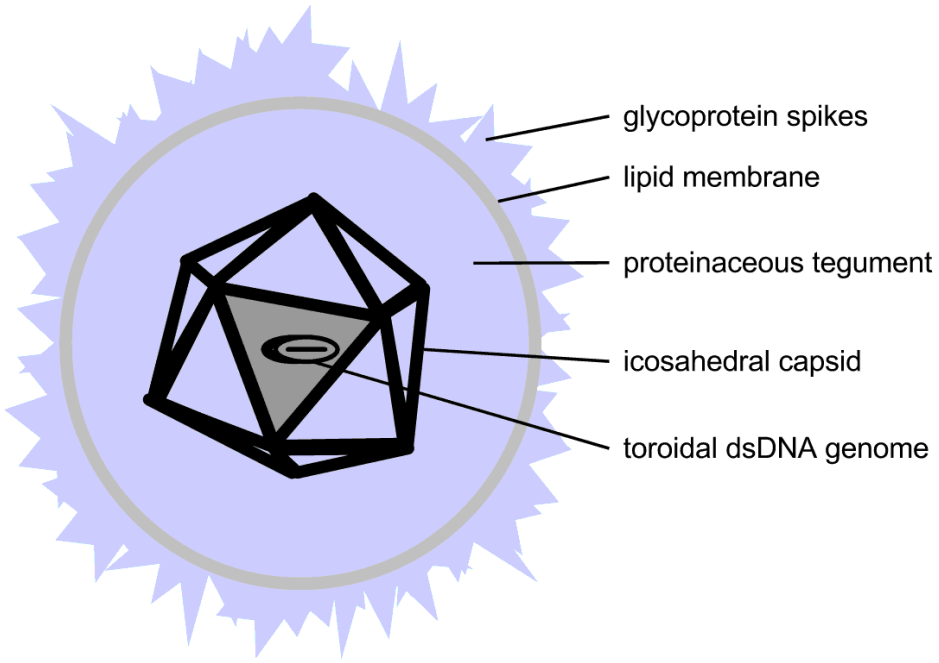

Figure 1-1. Graphic representation of herpesvirion. These virions are composed of a dsDNA genome packaged in an icosahedral nucleocapsid. The capsid is ensconced in a proteinaceous tegument layer and enveloped within a lipid membrane with glycoprotein spikes.

Herpesviruses are widely prevalent. More than two hundred

herpesviruses have been discovered thus far, and most metazoan species are host to at least one herpesvirus (Pellett and Roizman, 2007). A great degree of diversity accommodates this vast range of hosts. As such, *Herpesvirales* is the only virus taxon on the 'order' rank. The families under this order are: the *Malacoherpesviridae* family that includes the known bivalve herpesvirus; *Alloherpesviridae*, containing fish and amphibian herpesviruses; and *Herpesviridae* which describes avian, reptilian, and mammalian herpesviruses (McGeoch *et al*., 2006).

1.1.2 The *Herpesviridae* family

All *Herpesviridae* species share characteristics upon infection of a permissive cell (reviewed by Roizman *et al*., 2007). These species undertake DNA replication in the nucleus, using numerous nucleic acid-processing enzymes. Final assembly of their virions takes place in the cytoplasm. These viruses can establish latency in their hosts. Importantly, the viruses each encode protein-modifying enzymes. These species have been classified into subfamilies using biological characteristics, classification reaffirmed with nucleotide sequence data: *Alphaherpesvirinae*, *Betaherpesvirinae*, and *Gammaherpesvirinae* (reviewed by Roizman *et al*., 2007).

Viruses within *Gammaherpesvirinae* primarily infect lymphoblastoid cells in the family of their respective hosts, and typically establish latency in lymphoid tissue. *Betaherpesvirinae* species have a restricted host range and are prone to causing cytomegalia. These viruses have a long replication cycle and, as a result, spread slowly in tissue culture. Species of *Alphaherpesvirinae* are so classified for their wide host range, efficient destruction of infected cells with a short replication cycle, and consequent rapid spread in tissue culture. Alphaherpesviruses are neurotropic and capable of establishing latency in sensory ganglia.

Spanning these three subfamilies (Davison *et al*., 2009), there are

eight known human *Herpesviridae* viruses (reviewed by Ray and Ryan, 2010). Each has preferred tissues for primary and latent infection, and each is known by a taxonomic designation and often, but not always, by a common name (Davison *et al.*, 2009).

Gammaherpesviruses include *Human herpesvirus 4* and *Human herpesvirus 8*, commonly Epstein-Barr virus (EBV) and Kaposi's sarcoma-associated herpesvirus (KSHV) respectively (Davison *et al.*, 2009). EBV infects B lymphocytes, where it also establishes latency, possibly causing infectious mononucleosis and lymphocytic tumours (reviewed by Rickinson and Kieff, 2007). KSHV infects peripheral blood mononuclear cells (PBMCs) and is also tumorigenic, establishing latency in infected tumours (reviewed by Ganem, 2007).

Among *Betaherpesvirinae* species are *Human herpesvirus 5* (often called cytomegalovirus; CMV), *Human herpesvirus 6* (HHV-6), and *Human herpesvirus 7* (HHV-7) (Davison *et al.*, 2009). CMV infects lymphocytes and monocytes, going latent in various PBMCs and vascular endothelial tissue; CMV infection can cause acute systemic disorders in neonates or immunocompromised individuals, as well as some mononucleosis cases (reviewed by Mocarski *et al.*, 2007). HHV-6 and -7 both infect T cells and cause roseola (reviewed by Yamanishi *et al.*, 2007). While HHV-6 latently infects T cells, monocytes, and macrophages, HHV-7 only is latent in $CD4^+$ T cells.

Within *Alphaherpesvirinae* there are four genera: *Iltovirus*, *Mardivirus*, *Varicellovirus*, and *Simplexvirus* (Davison *et al.*, 2009). Primary infection with all human alphaherpesviruses is of epithelial tissues before lifelong ganglial latency. Varicellovirus *Human herpesvirus 3* is commonly called varicella-zoster virus and is the etiology of both chickenpox and shingles (reviewed by Cohen *et al.*, 2007). *Human herpesvirus 1* and *2* are simplexviruses commonly known as herpes simplex virus type 1 (HSV-1)

and 2 (HSV-2), respectively (Davison *et al.*, 2009). While these both cause skin lesions, the most notable difference between HSV-1 and -2 is the sites for which they are adapted to efficiently infect, HSV-2 preferring pubic sites, HSV-1 favouring facial sites (Engelberg *et al.*, 2003).

1.1.3 HSV-1 epidemiology and pathogenesis

HSV-1 is a ubiquitous human virus propagated by personal contact among its human hosts, the sole host reservoir for this virus. There are several established factors in HSV-1 prevalence. Host age and HSV-1 seroconversion are strongly correlated (Nahmias *et al.*, 1990; Smith and Robinson, 2002). This virus infects virtually every human by the end of his or her natural life span (Liedtke *et al.*, 1993; Inoue *et al.*, 2010; Smith and Robinson, 2002). Additionally, greater population density is a predictor of greater HSV-1 seroprevalence, as is commonly the case with crowding of developing nations or low-income housing in developed nations (Nahmias *et al.*, 1990), facilitating more frequent personal contact. Prevalence of HSV-1 is a function of geography, socioeconomic status, and age, factors that can increase opportunity for exposure and thus infection. Seroprevalence in Canada is about 50% on average of the population aged 15 to 44 years (Howard *et al.*, 2003).

Primary infection occurs at exposed epithelium: often dermal abrasions, oropharyngeal mucosa, or anogenital mucosa (Roizman *et al.*, 2007). Though infection is most often asymptomatic, the infection may present with mucosal ulceration or cutaneous vesicular lesions.

Depending on where symptomatic infection occurs, HSV-1 is known to cause several diseases (reviewed by Ray and Ryan, 2010; reviewed by Roizman *et al.*, 2007) whose symptoms usually resolve within 5 to 12 days. It is perhaps best known for causing orolabial herpes, orofacial lesions commonly called ‘cold sores’. Usually among children, it also causes viral

gingivostomatitis, painful oropharyngeal ulcers. When infection takes place at damaged skin, especially of hands and fingers, the resulting lesions are called herpetic whitlow. Symptomatic anogenital infection is genital herpes.

HSV-1 transmission can occur by any direct contact of infectious secretions with exposed epithelium, any touching that transfers infectious virions. In addition to symptomatic secretion, asymptomatic shedding (reviewed by Miller and Danaher, 2008) through saliva or tears is common and often responsible for transmission. Thus, it may not be readily apparent when one is infectious, nor when another is infected. Historically, most were infected by the age of 5 (Roizman *et al*., 2007), implying efficient vertical transmission from infected parents.

HSV-1 also causes sexually transmitted infections (STIs). Traditionally, sexual activity is not specifically enumerated as a factor in HSV-1 transmission. This attitude is exemplified by Smith and Robinson's (2002) reference to this virus as a "mainly non-STI". In reality, sexual behaviours are an important determinant of HSV-1 prevalence, causing a large subset of genital herpes. While HSV-2 was historically the primary cause of genital herpes and HSV-1 a minor cause, an inversion of that trend is apparent in younger demographics where HSV-1 is now the primary cause of genital herpes (Nilsen and Myrmel, 2000; Roberts *et al*., 2003). Further, oro-genital contact is linked to genital herpes caused by HSV-1 (Edwards and Carne, 1998; Lafferty *et al*., 2000), no doubt a consequence of oral asymptomatic shedding, and oral sex practices are increasingly common (Copen *et al*., 2012). This occupation of the HSV-2 niche of genital infection, coupled with evolving sexual behaviours, makes HSV-1 an increasingly relevant STI.

When primary infection spreads to adjacent sensory neurons, the virus establishes latency by retrograde axonal transport to a trigeminal ganglion from oral infection or the sacral ganglion from anogenital infection

(reviewed by Diefenbach *et al*., 2008). The virus intermittently reactivates from latency via anterograde axonal transport to sensory nerve endings (Huang *et al*., 2011), resuming its lytic infection usually at mucocutaneous sites. This is called recurrent infection and, though usually asymptomatic, may again result in vesicular lesions at these sites, and this is the mechanism behind recurrent orolabial herpes (Roizman *et al*, 2007).

This virus, through axonal transport, can potentially reactivate at any innervated site. In rare instances, such infections colonize the brain or the eye. Ocular infection causes corneal damage and can lead to blindness (reviewed by Tomi *et al*., 2008). HSV encephalitis occurs by migration to and infection of the temporoparietal region and has a 70% mortality rate if untreated (Whitley and Gnann, 2002).

Recurrence is not reliably predictable, but recurrence is associated with fever, the severity of the primary infection (Roizman *et al*., 2007), ultraviolet radiation exposure (Spruance *et al*., 1991), and periods of immunocompromisation (Segal *et al*., 1974; Ship *et al*., 1977).

Conditions and behaviours that promote contact and, therefore, exposure to HSV-1 are circumstances that enhance its transmission and prevalence. Diseases are a consequence of both the mode of transmission and the various stages of HSV-1 life cycle.

1.1.4 HSV-1 lytic replicative cycle

Progeny are generated by the virus's lytic cycle. Viral attachment proceeds by association of glycoprotein C (gC) (Harold *et al*., 1991) or gB (Harold *et al*., 1994) on the viral envelope to cellular glycosaminoglycans (Shieh *et al*., 1992). Viral gD subsequently binds nectins (Cocchi *et al*., 2000), herpesvirus entry mediator (Montgomery *et al*., 1996), or particular heparan sulfate species (Shukla *et al*., 1999) to trigger entry. The entry mechanism requires gH-gL heterodimerization and gB (Turner *et al*., 1998).

Membrane fusion exposes tegument to the cytosol. The nucleocapsid is transported to a nuclear pore while surrounding tegument proteins are gradually released, favouring outer tegument proteins (Granzow *et al.*, 2005). Once translocated to a nuclear pore by cellular dynein along the cellular microtubule network (Dohner *et al.*, 2002), the viral genome is ejected into the nucleus using virion protein 1/2 (Copeland *et al.*, 2009). In the nucleus, the genome circularizes.

Viral DNA replication and gene transcription are facilitated in the nucleus. Transcribed by host RNA polymerase II (Alwine *et al.*, 1974), viral gene expression is sequentially regulated. Based on this sequence, genes are grouped into four classes: α or immediate-early (IE) genes, required for efficient expression of all subsequent classes (Watson and Clements, 1978; Deluca *et al.*, 1985); β or early (E) genes, needed for viral DNA replication (Honess and Roizman, 1975); γ_1 leaky-late genes, whose expression is associated with viral genome replication; and γ_2 true-late genes, which strictly require viral DNA replication (Honess and Roizman, 1975).

Transcription of α genes requires virion protein 16 (VP16), which is packaged in the tegument of each virion; VP16 complexes with host factors HCF-1 then Oct-1 to bind DNA sequence TAATGARAT, inducing transcription from IE promoters (reviewed by Wysocka and Herr, 2003). The β genes, whose expression is potentiated by prior α expression, include genes that encode proteins for DNA replication, such as unique-long 9 (UL9) for an origin-binding protein, UL29 for a single-stranded DNA binding protein, UL5, UL8, and UL52 for the helicase-primase enzyme, and UL30 and UL42 for a polymerase (Roizman *et al.*, 2007). Concatemeric viral DNA is synthesized from the nuclear, circular viral genome. The γ gene class largely encodes structural proteins to be present in progeny virions, preparing for virion assembly and egress.

The prevailing model of assembly begins in the nucleus where the

concatemeric copies of the genome are processed into genomic units, each loaded into a capsid (reviewed by Roizman *et al.*, 2007). From the nucleus, the nucleocapsid translocates to the cytoplasm. This translocation entails envelopment and de-envelopment of the nucleocapsid through the nuclear membrane. The nucleocapsid is first enveloped at the inner nuclear membrane via laminar restructuring by viral proteins, encoded by UL31, UL34 (Reynolds *et al.*, 2004), and US3 (Reynolds *et al.*, 2002), and cellular protein kinase C (Park and Baines, 2006). This envelope is thought to fuse with the outer nuclear membrane using gB, gH (Farnsworth *et al.*, 2007), and US3 (Wisner *et al.*, 2009), discharging naked nucleocapsids into the cytoplasm. The capsid localizes to one of several cytoplasmic foci where tegumentation likely occurs (Nozawa *et al.*, 2004). The final envelope is acquired as the virion enters the Golgi apparatus, from which the complete virion is exocytosed (Stackpole, 1969).

1.1.5 HSV-1 latency: establishment and reactivation

When a primary infection reaches a sensory neuron, as outlined in subsection 1.1.3, this virus establishes latency when its nucleocapsid translocates to a ganglionic soma, localizing to a nuclear pore and ejecting its genome into the nucleus (reviewed by Held and Derfuss, 2011). From then until reactivation, the only robustly detectable viral expression is latency-associated transcript (LAT; Rock *et al.*, 1987), a non-coding viral RNA (Krause *et al.*, 1988), that antagonizes apoptosis by inhibiting caspase-8 and -9 (Henderson *et al.*, 2002). Precise conditions causing the re-initiation of lytic viral expression are not yet clear, but a number of observations have allowed for hypotheses explaining establishment, maintenance of, and reactivation from latency, where the role of LAT has been examined.

Within this neuronal nucleus, the viral genome associates with nucleosomal regions, suggesting a role for heterochromatic silencing in

latent-genome regulation (Deshmane and Fraser, 1989). Indeed, LAT was shown to chromatinize viral lytic gene regulation sequences (Wang *et al*., 2005), while the LAT gene remains euchromatic (Neumann *et al*., 2007) via histone modification (Kubat *et al*., 2004). In addition, neuronal expression of Oct-1 is weak relative to other cell types (Hagmann *et al*., 1995). This difference potentially allows Oct-1 to be competitively inhibited by close homologue Oct-2, stifling α-gene expression (Lillycrop *et al*., 1991). Dampened viral gene expression results from LAT expression, raising the possibility that LAT itself may be inhibiting viral genes (Garber *et al*., 1997). It has further been suggested that this latency is a *de facto* lytic infection that is severely attenuated by cell-mediated immunity (Liu *et al*., 2000; Simmons and Tscharke, 1992).

Reactivation can be induced by hyperthermic stress (Sawtell and Thompson, 1992). This stress induces expression of virion protein 16 (VP16), a necessary factor in reactivation (Thompson *et al*., 2009). The extent to which replication occurs and the abundance of ganglial latent genomes is correlated with frequency of reactivation (Sawtell 1998; Sawtell et al. 1998; Thompson and Sawtell 2000). This virus is only well adapted for reactivation from the trigeminal ganglion, as recurrent genital infection is relatively infrequent (Engelberg *et al*., 2003).

1.2 VIRAL MODULATION OF CELLULAR SIGNALLING MECHANISMS

1.2.1 PI3K-Akt signalling

Viruses have an interest in effecting conditions favourable for viral replication. Entirely dependent on the cell for viral protein synthesis, a virus modulates cellular translation enzymes. Beholden to cellular life for opportunity to replicate, a virus down-regulates apoptosis. Subject to the defence mechanisms of the broader organism, a virus employs immune evasion tactics. A common viral strategy in bringing about these outcomes

is manipulation of the phosphatidylinositol 3-kinase (PI3K)-Akt pathway. Among the viruses that use this strategy is HSV-1.

Independent from infection, host-endogenous factors regulate critical signalling events. Extracellular growth factors or cytokines ligate their cognate receptor tyrosine kinase, triggering dimerization or reorientation of its subunits and autophosphorylation of their intracellular tails (reviewed by Ottensmeyer *et al.*, 2000). Some receptors rely on other closely associated kinases, such as Src-family kinases (see subsection 1.2.3), for phosphorylation. Phosphotyrosine-containing sites in these intracellular tails serve to recruit signalling molecules, engaging a signalling cascade.

Phosphatidylinositol 3-kinase (PI3K) is a heterodimer of p110, the catalytic subunit, and p85, the regulatory subunit (reviewed by Vogt *et al.*, 2010). Shortly following receptor ligation, PI3K is localized to the plasma membrane by interacting with a receptor or receptor-bound adaptor molecule, such as IRS-1 (reviewed by Fantl *et al.*, 1993). PI3K then phosphorylates phosphatidylinositol 4,5-bisphosphate (PIP2) to produce an abundance of phosphatidylinositol 3,4,5-triphosphate (PIP3) on the plasma membrane inner leaflet (Auger *et al.*, 1989). Phosphatase and tensin homolog (PTEN) antagonizes this process by dephosphorylating PIP3 (Maehama and Dixon, 1998; Downes *et al.*, 2001). A PIP3-abundant plasma membrane recruits pleckstrin-homology (PH) domains. PH domain-containing proteins Akt and phosphoinositide-dependent protein kinase 1 (PDK1) co-localize at this PIP3-rich plasma membrane (Andjelkovic *et al.*, 1997; Calleja *et al.*, 2007). This facilitates the phosphorylation and activation of Akt by PDK1 phosphorylation on Akt Thr-308. Akt is further activated and phosphorylated at Ser-473 by what is currently thought to be mammalian target of rapamycin complex 2 (mTORC2; Facchinetti *et al.*, 2008). Akt, itself a serine/threonine kinase, can subsequently phosphorylate a wide array of downstream targets with anti-apoptotic,

pro-growth, and translation-enhancing effects.

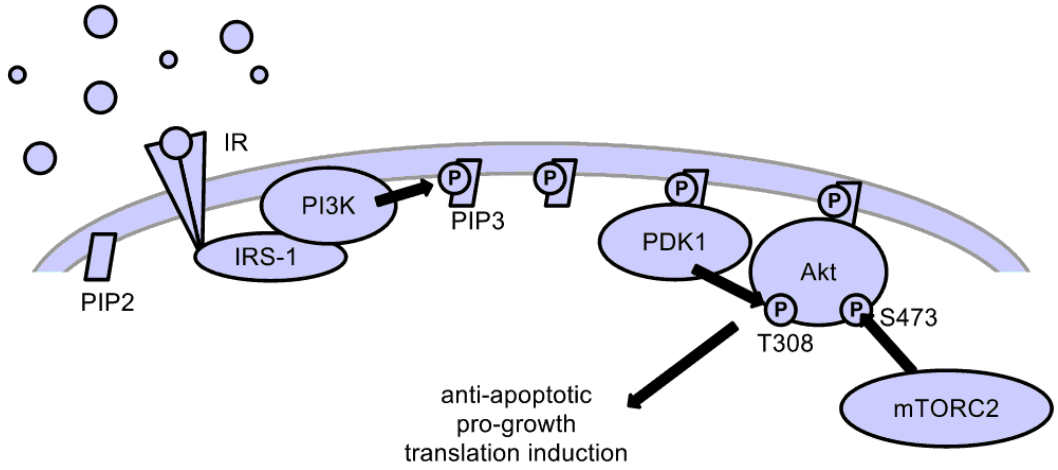

Figure 1-2. Initiation of PI3K-Akt signalling in the uninfected context. Receptor tyrosine kinases, such as insulin receptor (IR) pictured here, recruit and activate PI3K at the plasma membrane. IR requires an adaptor molecule, IRS-1, to do so. PI3K, a lipid kinase, generates PIP3 from PIP2. PIP3 facilitates the co-localization of PDK1 and Akt. PDK1 and mTORC2 phosphorylate Akt at Thr-308 and Ser-473 respectively. An activated Akt then induces several downstream pro-survival effects.

Akt signalling antagonizes apoptosis. Akt phosphorylates Bad (Datta *et al*., 1997), inactivating the Bcl-2-sequestering activity of Bad (reviewed by Danial, 2008). Bcl-2 can then bind pro-apoptotic Bcl-2-family proteins, preventing their dimerization and resultant pore formation on mitochondrial membranes (reviewed by Reed, 1998). In inactivating Bad, Akt enables Bcl-2 action to inhibit mitochondrial permeabilization. Akt phosphorylates Caspase-9 (Cardone *et al*, 1998). This modification inhibits Caspase-9 proteolytic activity and therefore its activation of executioner caspases. Further, Akt phosphorylates FOXO transcription factors (Burgerin and Medema, 2003), preventing their translocation to the nucleus for transcription of Fas ligand and Bim genes. Thus, Akt counteracts several crucial events in mitochondrion-dependent and -independent apoptotic signalling.

Akt phosphorylation of some effectors also promotes growth and cell cycle progression. For example, Akt phosphorylates p21 (Rössig *et al.*, 2001), a key inhibitor of cyclin-dependent kinases (CDK). Upon phosphorylation, p21 is inhibited and can no longer complex with cyclins and CDKs (Harper *et al.*, 1993). This deregulates cell cycle checkpoints and enhances cell cycle progression. Akt also phosphorylates and inhibits AMPK (Hahn-Windgassen *et al.*, 2005), resulting in up-regulation of various metabolic pathways.

Akt potentiates cellular protein synthesis activity. By phosphorylating and inactivating TSC2 (Gao and Pan, 2001; Manning *et al.*, 2002), Akt activates mTORC1 and, consequently, S6K (reviewed by Wullschleger *et al.*, 2006). An activated S6K can then phosphorylate rpS6 (reviewed by Ruvinsky and Meyuhas, 2006), inducing translation. Active mTORC1 also phosphorylates 4E-BP1 to inhibit its translational antagonism and promote translation (reviewed by Wullschleger *et al.*, 2006).

Signal transduction through Akt results in activation of numerous factors that favour the prerequisite conditions for viral replication. Every virus is completely dependent on host cell processes for protein synthesis, and Akt signalling activates translation machinery. For a virus to sustainably consume materials within a cell, the cell necessarily must metabolize more materials for virus use, and Akt effectors enhance metabolism. Akt secures necessities for any viral life cycle.

Also benefiting viruses, Akt activation antagonizes antiviral innate immunity. Secreted in response to viral nucleic acid-detection with a wide range of pleiotropic effects, interferon-β (IFN-β) also triggers pro-apoptotic signalling (Lokshin *et al.*, 1995). As Akt effectors intersect apoptotic signalling at multiple points (Lei *et al.*, 2005), Akt signalling antagonizes that of IFN-β.

Viral induction of Akt pathways is a strategy for viruses to extend

cellular life and opportunity for viral replication, as well as facilitate conditions favourable for a virus life cycle, namely elevated metabolism and up-regulated translation. Indeed, a multitude of viruses, including herpesviruses, modulate Akt signalling pathways to that end.

1.2.2 Viral activation of Akt signalling

The various instances of viral Akt signalling modulation can be described thus: how the virus alters the kinetics of a given step in signal transduction; and where the altered step is along the PI3K-Akt axis.

Viruses encode viral homologues of cellular signalling molecules. In fact, cellular Akt was first discovered as a homologue of viral protein v-Akt of murine retrovirus AKT8 (Bellacosa *et al.*, 1991). This v-Akt allows the virus to drive flux downstream of Akt, bypassing cellular Akt activation, and is a key exemplar of molecular mimicry as a modulation mechanism.

Viruses also encode proteins that bind cell-endogenous signalling modulators. Myxoma virus expresses ankyrin-repeat protein M-T5, a molecule that binds Akt and promotes its activation (Wang *et al.*, 2006). Cytomegalovirus (CMV) protein UL38 binds TSC2, an mTOR inhibitor (Moorman *et al.*, 2008). In the uninfected context, an activated Akt phosphorylates TSC2 to prevent its inhibition of mTOR. CMV infection inactivates TSC2 via UL38, indirectly activating mTOR complexes and protein synthesis. Thus, protein-protein interactions for either induced activation or sequestration are a means by which viruses exert their influence on Akt effectors. Notably, viral protein-modifying enzymes also play a role. HSV-1 US3 kinase phosphorylates and activates a subset of Akt effectors (described further in section 1.3).

Taken together, we see that mimicry of and direct interaction with host factors are mechanisms by which Akt signal flux is enhanced. The other key consideration is where this enhancement occurs. Upstream of

Akt, multiple activatory signals converge at PI3K. At Akt, the signal diverges to influence a wide variety of effectors with various functions and outcomes.

Therefore, all other things being equal, a single enhancement of signal transduction upstream of Akt globally enhances Akt effector pathways, and a downstream enhancement promotes only a subset of Akt effector pathways (barring signals that reach mTORC2, which create positive feedback by assisting in Akt phosphorylation). For example, Influenza A virus expresses protein NS1, whose role includes binding p85, activating PI3K (Hale *et al.*, 2006). NS1-induced modulation, upstream of Akt, cannot discriminate among Akt effectors. In contrast, Hepatitis C virus protein NS5A inactivates FKBP38 (Peng *et al.*, 2010), an mTOR down-regulator (Bai *et al.*, 2007). As such, NS5A selectively induces Akt effectors.

While the numerous viruses that induce Akt signalling are not limited to those mentioned, the examples described here serve to illustrate the variety of mechanisms by which viruses induce Akt signalling. It is further important to consider those factors that signal into Akt upstream of PI3K, which are not limited to receptor tyrosine kinases.

1.2.3 Src-family kinases and Src-homology domains in signalling

One set of enzymes capable of upstream action in PI3K-Akt signalling is the Src-family protein tyrosine kinases (SFK; Figure 1-3). For example, the SFK Lck phosphorylates p85 to induce PI3K activation (von Willebrand *et al.*, 1994; Cuevas *et al.*, 1999). SFKs are major players in growth signalling, due to their phosphorylation of numerous tyrosine-containing motifs, facilitating the complexing of signalling adaptor proteins such as IRS-1 (Amanchy *et al.*, 2009). SFKs are so named for Src, the prototypical SFK identified by its homology with the namesake Rous sarcoma virus kinase linked to transformation (Stehelin *et al.*, 1976).

SFKs are constitutively targeted to the plasma membrane via

amino-terminal myristoyl and palmitoyl modifications (Koegl *et al.*, 1994; reviewed by Resh, 1999). Src-homology 2 (SH2) and Src-homology 3 (SH3) domains mediate interactions with either the carboxy terminus of the SFK itself or activating proteins (Figure 1-3). SH2 and SH3 domains bind phosphotyrosyl motifs and polyproline motifs, respectively, and such homologous domains are present in numerous signalling proteins among numerous pathways (reviewed by Pawson and Scott, 1997; reviewed by Pawson and Nash, 2000).

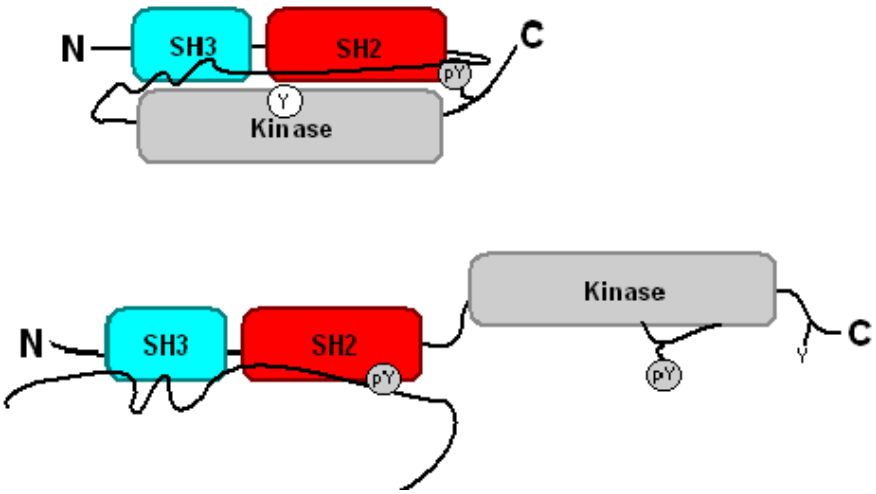

Figure 1-3. Model of src-family kinase activation. Phosphorylation of the inhibitory C-terminal tyrosine by Csk mediates a closed conformation through interaction with the SH2 domain (top). Dephosphorylation of the C-terminal tyrosine allows for the open and active conformation. The open conformation allows for the activatory tyrosine to be phosphorylated, stabilizing the open conformation regardless of the phosphorylation state of the inhibitory tyrosine. Src-family kinases can also be opened and activated if another protein out-competes the C terminus for interaction (bottom).

SFK activity is strictly regulated via conformational changes, normally brought about by the phosphorylation states of two tyrosine residues (Sicheri and Kuriyan, 1997). When the carboxy-terminal inhibitory tyrosine is phosphorylated, this phosphotyrosine binds the SH2 domain, forcing the

SFK into an inactive closed conformation; SH3 interactions stabilize this conformation (Figure 1-3; Sicheri *et al.*, 1997; Williams *et al.*, 1997; Xu *et al.*, 1997). This tyrosine is phosphorylated by C-terminal Src kinase (Csk; Nada *et al.*, 1991). CD45 phosphatase, on the other hand, dephosphorylates this residue, maintaining an open active SFK conformation (Ostergaard *et al.*, 1989). Once in an open conformation, the activatory tyrosine may be phosphorylated, disrupting an α-helical loop that would otherwise obscure the catalytic cleft; this activatory tyrosine phosphorylation enhances enzymatic activity (Veillette and Fournel, 1990).

Intermolecular interactions can also induce an open and active conformation in SFKs (Burnham *et al.*, 2000; Bromann *et al.*, 2004; Thomas *et al.*, 1998). A theme observed in exogenous SFK activation is SH2- and SH3-domain interactions that outcompete intramolecular interactions with its C terminus.

Associations with SH domains are dependent on the primary structure of the interacting protein (reviewed by Kuriyan and Cowburn, 1997). Each SH domain mediates protein-protein interactions with a specificity for a particular amino acid motif. This specificity is dictated by residues proximal to the binding groove of the domain. However, while SH2 domains all bind phosphotyrosyl motifs, not all SH2 domains bind exactly the same motif. SH2 domains among various proteins are closely homologous, but there are various preferred sequences for their respective associations (Songyang *et al.*, 1993).

A protein exposing the preferred SH2 binding motif of SFK SH2 domains, phospho (p)-Tyr-Glu-Glu-Ile, may outcompete the inhibitory tyrosine and allow an open SFK conformation (Songyang *et al.*, 1993). PI3K recruitment to a signalling complex depends on binding to a pTyr-Xxx-Xxx-Met motif by an SH2 domain of p85, the PI3K regulatory subunit (Songyang *et al.*, 1993). SH2 associations are dependent on the

tyrosine phosphorylation and the following three residues, each category of SH2 domains preferring a different adjacent sequence (Waksman *et al.*, 1993). Once this association is in place, the catalytic subunit p110 phosphorylates lipids to produce PIP3.

1.2.4 Viral induction of Src-family kinase

SFKs are likewise subject to manipulation by viral proteins. HSV-1 protein infected cell polypeptide 0 interacts with Src SH3 domains resulting in Src activation (Liang and Roizman, 2006). Influenza A entry induces SFK Syk activation (Lau *et al.*, 2008). Polyoma virus middle T antigen (mTAg), while participating in neither SH2 nor SH3 interaction, binds to the Src C-terminal region to induce its activation (Dunant *et al.*, 1996). An activated SFK is consequently free to phosphorylate Tyr residues creating binding sites for signalling molecules, events analogous with autophosphorylation of an RTK.

Viruses leverage interactions with multiple binding partners along the PI3K-Akt axis to bypass endogenous host-induced signalling initiation in favour of a virus-induced signalling programmes. Each of these tactics exemplifies a strategy for induction of growth conditions favourable to the virus.

1.3 TEGUMENT PROTEINS OF INTEREST

1.3.1 Advantages of tegumentation

The proteins of interest here have been shown to modulate PI3K-Akt signalling and, interestingly, are tegument proteins. Unique to herpesviruses, a complement of tegument proteins accompanies each virion and is fully manufactured before infection. As explained in subsection 1.1.4, attachment and entry of a virion to a host cell entails exposure and diffusion of the tegument in the cytosolic compartment. Thus, even before the viral

gene expression program is engaged, tegument proteins are poised for immediate action upon cell signalling. Moreover, the manufacture of tegument proteins necessary for virion assembly ensures an abundance of cytosolic tegument proteins late in the lytic cycle. The tegument proteins may be relevant to cell signalling effects in this context as well. There is evidence for two HSV-1 tegument proteins to potentially play a role in this fashion via their modulation of PI3K-Akt signalling: unique-short 3 (US3) protein kinase, and virion protein 11/12 (VP11/12).

1.3.2 US3 protein kinase

Of the two, much more is known of US3 protein kinase (US3PK), a serine/threonine protein kinase. Encoded by gene US3, US3PK is an extremely versatile kinase that modifies a wide range of substrates.

Among the most notable of US3PK functions are the assistance in capsid egress, relief of chromatinization, and subversion of host apoptotic regulation. Two viral proteins considered necessary for capsid budding at the inner nuclear membrane are the products of genes UL31 and UL34, which complex at the inner nuclear membrane. As observed in US3-null infection, without phosphorylation by US3PK (Mou *et al*., 2009; Purves *et al*., 1991) the UL31-UL34 complexes are unevenly distributed and aggregate into distinct foci, presumably hindering their function (Kato *et al*., 2006). Histone deacetylases (HDAC) remove acetyl groups from histone lysine residues, which results in heterochromatin formation. US3PK phosphorylates HDAC 1 and 2, inactivating their enzymatic activity, loosening chromatin structure and enhancing gene expression (Walters *et al*., 2010). In cell-mediated immunity, cytotoxic T lymphocytes release granzyme B to targeted cells, resulting in Bid cleavage and apoptotic induction. US3PK also phosphorylates Bid, preventing its cleavage by granzyme B and subsequent induction of apoptosis (Cartier *et al*., 2003).

US3PK phosphorylates Bad to block mitochondrion-dependent apoptotic signalling (Munger and Roizman, 2001), acting much as Akt does (subsection 1.2.1).

Recent investigation by the Mohr group has illuminated further aspects of US3PK function that overlap with that of Akt (Chuluunbaatar *et al.*, 2010). US3PK acts on multiple Akt effectors, requiring no action of Akt itself, with no amino acid sequence identity with Akt. US3PK phosphorylates TSC2 at Ser-939 and Thr-1462, identical to those residues phosphorylated by Akt. These modifications promote mTORC1 activation and translation. FOXO1, transcription factor to pro-apoptotic genes, is phosphorylated and inactivated by US3PK by modification on the same residues that Akt targets. GSK3, a positive regulator of p53, is also inactivated by US3PK phosphorylation at Akt-regulated residues. In bypassing Akt, US3PK allows HSV-1 to selectively activate pro-viral effectors without reliance on more cellular factors.

US3PK also influences the Akt phosphorylation state. US3PK-null mutants were shown to have enhanced Akt activation, implying that US3PK inhibits Akt activation (Benetti and Roizman, 2006). Importantly, US3PK is also necessary for the stabilization of VP11/12 among HSV-2 orthologues (Matsuzaki *et al.*, 2005).

1.3.3 Virion protein 11/12

VP11/12 is one of the most abundant tegument proteins and is encoded by the unique-long 46 (UL46) gene. This phosphoprotein is membrane-associated and localizes to either the plasma membrane or perinuclear sites of virion assembly (Kato *et al.*, 2000). VP11/12 was shown to potentiate virion protein 16 (VP16)-mediated viral immediate-early expression in a transient transfection model (McKnight *et al.*, 1987). Agreeing with this observation, VP11/12 interacts with VP16 (Zhang *et al.*,

1991). UL46-null mutants, however, are viable in cell culture and do not show defective IE transcription (Zahariadis *et al.*, 2008). Given this, it is inferred that the primary role of VP11/12 remains to be discovered. That function would remain completely enigmatic until recent observations.

Analyses of virion protein 11/12 post-translational modifications and interactions by Melany Wagner (former doctoral candidate of the Smiley lab and PhD alumna of University of Alberta) allow for the generation of a working model. The Smiley laboratory, which I hereinafter call 'the lab', showed that VP11/12 is heavily tyrosine-phosphorylated in infected Jurkat T cells (Zahariadis *et al.*, 2008). This phenomenon is cell type-dependent. Phosphotyrosine levels are abrogated in the presence of the small-molecule SFK inhibitor PP2, suggesting that the phosphorylation is SFK-dependent. In JCAM1.6, an *lck*-deleted Jurkat-derived cell line, VP11/12 tyrosine phosphorylation appears strongly inhibited but still detectable, implying that Lck is required for efficient VP11/12 tyrosine phosphorylation (Zahariadis *et al.*, 2008). VP11/12 can thus use other SFKs for tyrosine phosphorylation, and Lck is not strictly necessary for this effect. VP11/12 and Lck co-immunoprecipitate, demonstrating a physical interaction (Wagner and Smiley, 2009). The hypothesis that Lck phosphorylates VP11/12 is consistent with these observations. The lab has shown that VP11/12 and p85 co-immunoprecipitate as well (Wagner and Smiley, 2011). VP11/12 interaction with p85 is SFK-dependent as PP2 inhibition of SFKs inhibits association (Wagner and Smiley, 2011). HSV-1 activates Lck and PI3K, and VP11/12 is required these activations (Wagner and Smiley, 2011). Interestingly, VP11/12 amino acid sequence includes a tyrosine-containing motif predicted, upon phosphorylation, to interact strongly with the SH2 domain of Lck, YEEI.

Wagner and Smiley proposed a model. VP11/12 is hypothesized to use its phosphotyrosyl moiety at positions 624 through 627, YEEI, to bind

Lck, inducing its activation (Wagner and Smiley, 2009). This then closely associated kinase then could phosphorylate other VP11/12 tyrosyl motifs, completing the binding site for PI3K regulatory subunit p85, YTHM (Wagner and Smiley, 2011), and other signalling molecules. This proposed mechanism explains PI3K activation and resultant Akt activation.

1.3.4 Rationale for described studies

The initiating interaction of the Wagner-Smiley model is that between VP11/12 and Lck. The model implies that phospho-YEEI on VP11/12 mediates its activatory interaction with the SH2 domain of Lck, out-competing its carboxy-terminal inhibitory phospho-sequence. Chapter 3 describes *in silico* investigation and *in vitro* assays to test the necessary first step of this model.

To further explore the lab's interest in VP11/12, likely regulators of VP11/12 are of keen interest. Thus, US3PK is of particular interest. Studies of close orthologues of US3PK and VP11/12 show US3PK enhancement of VP11/12 stability (Matsuzaki *et al.*, 2005). If we infer an analogous interaction in HSV-1 infection, this observation is seemingly at odds with the finding that US3PK inhibits Akt activation (Benetti and Roizman, 2006). Further investigation to reconcile these two observations requires a panel of UL46- and US3-null single and double knock-outs from the same parental strain. Chapter 4 describes how US3-null mutants were generated, and outlines some preliminary characterization of these mutants.

Chapter II

Materials and Methods

2.1 MAMMALIAN CELLS AND CULTURE MEDIA

Jurkat 6.8 T cells were donated by Dr. Hanne Ostergaard, originally obtained from the ATCC (Goldsmith and Weiss, 1987). Jurkat cells were cultured in Gibco RPMI 1640 supplemented with 10% fetal bovine serum (FBS), 200 mM L-glutamine, 100 mM sodium pyruvate, and 100 U/ml penicillin-streptomycin. Vero immortalized monkey kidney epithelial cells and human embryonic lung (HEL) primary fibroblasts were procured from the ATCC. Cre-Vero, a Vero-derived cell line stably transfected to express Cre, was previously described (Geirasch *et al.*, 2006). HEL fibroblasts were grown in Gibco Dulbecco's modified Eagle's medium (DMEM) supplemented with 10% FBS, 100 mM sodium pyruvate, and 100 U/ml penicillin-streptomycin. Vero cells were cultured in Gibco DMEM supplemented with 5% FBS and 100 U/ml penicillin-streptomycin. Cells were cultured at 37°C and 5% CO_2 in a humidified chamber.

2.2 VIRUSES AND VIRUS-ENCODING BACMIDS

HSV-1 KOS-derived recombinants, KOS-G (Minaker *et al.*, 2005) and GHSV-UL46 (Willard, 2002), were described previously. HSV-1 strain F and mutants derived from strain F, R7041 (US3-null) and R7306 (US3-rescued) (Purves *et al.*, 1987), were provided by Dr. Bernard Roizman (University of Chicago, Chicago, IL, USA).

KOS-37 is a KOS-derived BACmid that encodes the HSV-1 genome containing BAC elements in the UL37-UL38 intergenic region for maintenance in bacteria (Gierasch *et al.*, 2006). The BAC elements are floxed, flanked by *loxP* sites, regions of specific recognition and efficient recombination mediated by Cre recombinase. Thus, Cre recombinase

mediates homologous recombination between *loxP* sites, excising the interposing sequence in Cre-expressing cells. The KOS-37 BACmid was a gift from Dr. David Leib (Washington University in St. Louis, St. Louis, MO, USA; currently at Dartmouth College, Hanover, NH, USA). The construction of the KOS-37-derived UL46-null BACmid by the lab was described previously (Zahariadis *et al*., 2008).

Virus stocks were generated by low-multiplicity infection (section 2.12) of Vero cells and incubation to total cytopathic effect. Cells were then pelleted at 4°C and resuspended in serum-free medium. Lysis was performed by freeze-thaw, 3 times, and cup-horn sonication on ice until homogenous. Cell debris was cleared by centrifugation.

Virus titre was determined by plaque assay on confluent Vero cells. Serial dilutions of virus stock were used for infection (section 2.12) in duplicate. Serum-supplemented incubation, however, was performed with a 1% human serum (instead of 5% fetal bovine serum) supplementation. When plaques were identifiable under light microscope, cells were fixed with methanol and Geimsa-stained. Plaques were counted and averaged between duplicate infections to measure titre in plaque-forming units (PFU) per volume of stock.

2.3 PLASMIDS

An empty pGEX vector (GE Healthcare Life Sciences) was used to express the glutathione S-transferase (GST) tag. A pGEX-derived plasmid expressing GST fused to the SH2 domain of Lck generated by Veillette *et al*. (1992) and given to the lab by Dr. André Veillette (University of Montréal, Montréal, QC, Canada); the resultant fusion protein expression is referred to here as GST-SH2(Lck).

2.4 SYNTHETIC PEPTIDES

Peptides were ordered from and manufactured by CanPeptide (Pointe-Claire, QC, Canada) to a reported purity of ≥90% (Table 2-1). Each have N-terminal biotinylations.

Table 2-1. Synthetic polypeptides.

Sequence and Modifications	Source and GenBank Accession (range)	CanPeptide Catalog No.
biotin-GGRV(**p**)YEEIPWMR	VP11/12 NP_044648.1 (620..631)	CP08875
biotin-GGRVYEEIPWMR	VP11/12 NP_044648.1 (620..631)	CP08954
biotin-PATY(**p**)YTHMGEVP	VP11/12 NP_044648.1 (515..526)	CP08876
biotin-FTATEGQ(**p**)YQPQP	human Lck NP_005347.3 (498..509)	CP09045

Phosphoryl modifications are denoted by a parenthesized and bolded lowercase letter '**p**' *preceding* the phosphorylated residue.

2.5 SYNTHETIC OLIGONUCLEOTIDES

Oligonucleotides were manufactured by Integrated DNA Technologies (Coralville, IA, USA) (Table 2-2).

Table 2-2. Synthetic oligonucleotides.

Name	Sequence (5' to 3')	Reference Sequence and GenBank Accession		Oligo Homology to Reference Sequence
JRS3	GCGTGATGTCACCATTGAAG	pgalK	FR832405.1	808..827
JRS4	CACTGTCCTGCTCCTTGTGA	pgalK	FR832405.1	1219..1200
JRS596	CGGGGCCCGTCGTTCGG	US3	NC_001806.1	135172..135188
JRS597	TCGGGGTCTTTTTGTGCCAACCCG	US3	NC_001806.1	136717..136694
JRS599	CAAACCTTCCCACACCACACCACCC AGCGAGGCCGAGCGCCTGTGTCATC **CCTGTTGACAATTAATCATCGGCA**	US3 **pgalK**	NC_001806.1 **FR832405.1**	135381..135430 **1..24**
JRS600	AAGATCACCAGACCGGCGCTCCAAA TGTCGACGGTCGTGGTATACGGATC	US3	NC_001806.1	136339..136290

	TCAGCACTGTCCTGCTCCTT	**pgalK**	**FR832405.1**	**1231..1212**
JRS611	CAAACCTTCCCACACCACACCACCC GGCGATGCCGAGCGCCTGTGTCATC	US3	NC_001806.1	135381..135430
	GATCCGTATACCACGACCGTCGACA TTTGGAGCGCCGGTCTGGTGATCTT	**US3**	**NC_001806.1**	**136290..136339**
JRS612	AAGATCACCAGACCGGCGCTCCAAA TGTCGACGGTCGTGGTATACGGATC	US3	NC_001806.1	136339..136290
	GATGACACAGGCGCTCGGCATCGCC GGGTGGTGTGGTGTGGGAAGGTTTG	**US3**	**NC_001806.1**	**135430..135381**

Bolded font face differentiates sequence of 3' ends that is not homologous to contiguous sequence.

2.6 INFORMATICS

2.6.1 Finding putative binding motifs

The ScanSite 2.0 search algorithm MotifScan (Obenauer *et al.*, 2003) and Eukaryotic Linear Motif (ELM; Puntervoll *et al.*, 2003) search tool were used to query HSV-1 VP11/12 amino acid sequence (accession no. NP_044648.1) for possible binding motifs. Consensus hits from both MotifScan and ELM were identified.

2.6.2 Multiple sequence alignment

Amino acid sequences from HSV-1 VP11/12 and orthologues were found by using Position-Specific Iterative (PSI)-Basic Local Alignment Search Tool (BLAST) (Altschul and Koonin, 1998) and HSV-1 VP11/12 (accession no. NP_044648.1) as the query sequence. The hits were aligned with Multiple Alignment using Fast Fourier Transform (MAFFT; Katoh *et al.*, 2002). Conservation of consensus binding motif hits (described in the prior subsection) was visually assessed on the multiple sequence alignment.

2.7 EXPRESSION AND PURIFICATION OF GST PROTEINS

GST lysis and binding (GLAB) buffer was used to solubilize GST protein for binding assays and is composed of 1% Triton X-100, 20 mM

Tris-Cl (pH 8.0), 137 mM NaCl, 2 mM EDTA (pH 8.0), 1X Roche complete (a protease inhibitor cocktail), 5 mM 2-ME (to keep glutathione reduced). In cases where GLAB buffer was used to prepare Jurkat cell lysate for interaction assays, the buffer was supplemented with the following phosphatase inhibitors at these concentrations: 10 mM β-glycerophosphate, 10 mM NaF, and 1 mM Na_3VO_4.

E. coli BL21 harbouring plasmids encoding GST proteins were grown in liquid culture. Starter cultures of 5 ml were grown overnight at 37°C with agitation in Luria-Burtani (LB) broth supplemented with 100 µg/ml ampicillin. Large-scale cultures of 100 or 200 ml were grown by inoculation with the starter culture at 1:500 (inoculum:LB) and incubation at 37°C with agitation until the OD_{600} measured 0.6. The pGEX expression system was then induced with isopropyl β-D-1-thiogalactopyranoside at 1 mM. The cultures were then incubated at 30°C for 3 h, after which the bacteria were pelleted at 3,000 × *g* for 20 min at 4°C. The pellet was resuspended in GLAB buffer (10 ml buffer per 100 ml culture-equivalent pellet) and lysis was allowed to proceed for 10 min at 4°C before storage at -20°C. Lysates were thawed on ice and sonicated on ice using a microtip horn until homogenized. Lysates were then cleared at 15,000 × *g* for 30 min at 4°C.

Clarified lysates were incubated with glutathione-agarose beads (Sigma G4510; about 1 ml packed beads per 10 ml lysate) with inversion mixing at 4°C for at least 1 h. Beads were washed thrice with GLAB buffer and twice with phosphate-buffered saline (PBS). Beads were stored as a 10% (v/v) slurry in PBS with 0.02% NaN_3 as a preservative at 4°C.

2.8 QUANTITATION OF GST PROTEIN

2.8.1 Soluble

GST protein was eluted from beads using GLAB buffer with 20 mM reduced glutathione as the eluant. To quantitate the protein content of the

eluate, a Bradford assay was performed using Bio-rad Protein Assay reagent at the manufacturer-specified concentration and conditions. This soluble protein was subsequently used in peptide pull-down experiments.

2.8.2 Bead-immobilized

Bead-GST protein suspensions were boiled in SDS lysis buffer for 5 minutes, resolved by 12% SDS-PAGE with bovine serum albumin (BSA) standards, and transferred onto a nitrocellulose membrane. The membrane was stained with Ponceau S. An estimation of the quantity of protein per volume of slurry was obtained visually by comparison with BSA standards.

2.9 PEPTIDE PULL-DOWN

2.9.1 Calculated molar binding capacity of streptavidin-agarose resin

Streptavidin-agarose (SA) beads (Sigma S1638) were used to immobilize mono-biotinylated peptides (Table 2-1) for peptide-protein interaction assays. To control for the quantity of peptide bound to each bed of resin, I sought an accurate estimation of the molar binding capacity of that resin. Sigma literature specifies S1638 capacity as "≥15 µg/mL binding capacity (biotin)." The specifications do not explicitly state whether this is the capacity of packed beads or of the suspension in which the product is shipped. Given precedent set by other Sigma resin-conjugate products with more detailed online specifications, I assumed the capacity is given per volume of packed beads, not slurry. Subject to the imprecise range of the specified value, I assumed a 20 µg/ml biotin binding capacity.

$$MM_{biotin} = 244.31\ g \cdot mol^{-1} \quad capacity_{biotin} = 2 \times 10^{-5}\ g \cdot ml^{-1}$$

$$molarcapacity_{biotin} = \frac{2 \times 10^{-5}\, g \cdot ml^{-1}}{244.31\, g \cdot mol^{-1}}$$
$$= 8.187 \times 10^{-8}\, mol \cdot ml^{-1}$$
$$\approx \mathbf{8 \times 10^{-8}\, mol \cdot ml^{-1}}$$

The biotin (and for our interests, peptide) binding capacity of the streptavidin-agarose (SA) packed beads is 8 x 10^{-8} mol/ml.

2.9.2 Adhering peptide to streptavidin-agarose beads

To probe clarified Jurkat cell lysate for full-length Lck, 1 nmol of peptide was used. To capture 1 nmol of mono-biotinylated peptide, 12.5 µl of packed SA beads were necessary.

$$V_{packedSA} = \frac{1 \times 10^{-9}\, mol}{8 \times 10^{-8}\, mol \cdot ml^{-1}}$$
$$= 0.0125\, ml$$
$$= 12.5\, \mu l$$

To probe purified GST-SH2(Lck) and GST solution, 2 pmol of peptide were used. Likewise, to immobilize 2 pmol of peptide, 0.025 µl of packed beads were necessary.

$$V_{packedSA} = \frac{2 \times 10^{-12}\, mol}{8 \times 10^{-8}\, mol \cdot ml^{-1}}$$
$$= 0.000025\, ml$$
$$= 0.025\, \mu l$$

SA beads required here were of such miniscule quantities that several considerations were observed to minimize experimental error. Pipettes that measured the lowest volumes were not sufficient to transfer

some desired bead quantities, and without sufficiently dilute slurries pipetting error would give rise to experimental error in the amounts of immobilized peptide used. Thus, serial dilutions were necessary to obtain the minute amounts of beads desired. Any instance wherein error in small-quantity bead-suspension transfer is experimentally meaningful is when pipetting error is the foremost consideration. Further, particularly in serially diluting the SA beads, meaningful disparities in bead amounts could indeed accrue due to error in pipetting heterogeneous suspensions and volume error. Therefore, thorough and vigilant vortexing of slurries immediately in advance of each slurry transfer was executed throughout experiments involving small quantities of SA beads. Given the multitude of opportunities for experimental error due to SA bead transfer, batch preparation was foregone in favour of *ad hoc* preparation for each replicate of each experiment. In this fashion, no one preparation of immobilized peptide would influence multiple experiments or experimental replicates, and each replicate of each experiment would serve as a more independent verification of each observation. Hence, in advance of each experimental trial, the quantities of immobilized peptide necessary for that experiment were prepared.

Microfuge tubes with aliquots of about 200 µl PBS were prepared. Desired mass of SA beads were transferred into these tubes, using the PBS to rinse the pipette tip for residual beads, from well agitated SA dilutions that allowed the accurate measurement of the desired volume of beads. Slurry containing 100 µl of Sepharose CL-4B (Sigma CL4B200) packed beads was transferred into each tube to act as carrier beads, as experimentally significant amounts of beads would be lost in subsequent washes without carrier beads. The suspensions were vortexed until well homogenized before beads were pelleted by centrifugation and supernatants removed. Five hundred µl of PBS were added to each bed of

beads. A quantity of peptide at least twice the molar capacity of the present SA beads were added to each slurry, and the suspensions were incubated at room temperature for 15 minutes with inversion mixing. The beads were then washed 4 times with 4°C PBS.

2.9.3 Incubation and precipitation

For assays involving soluble GST proteins, protein was diluted to 4 µM in GLAB buffer. Molar masses were assumed to be 26,000 g/mol for GST and 46,000 g/mol for GST-SH2(Lck). In these assays, 1 nmol of GST protein (or 250 µl of solution) was used.

Resin was pelleted and supernatants removed. Solution containing candidate binding partner protein was applied to resin-immobilized peptide, and incubated with inversion mixing overnight. Beads were then pelleted and washed 5 times in PBS at 4°C, and 100 µl PBS were added for SDS-PAGE.

2.10 JURKAT INFECTION

Jurkat cells were infected at a multiplicity of infection (MOI) of 10 plaque-forming units (PFU) per cell in culture medium lacking FBS at a cell concentration of 1×10^6 cells per 100 µl, humidified at 37°C for 1 h. At 1 hpi, the cells were allowed to recover in full FBS-supplemented culture medium for the remainder of each 13 h infection in a humidified 37°C chamber at a cell concentration of 1×10^6 cells per ml.

2.11 GST PULL-DOWN

Infected Jurkat cells were harvested at 13 h. Cells were chilled on ice and washed with PBS. Lysis was performed at a concentration of 1×10^6 cells per 100 µl buffer on ice in GLAB buffer with phosphatase inhibitors. Infected Jurkat cell lysates were cleared by centrifugation at 15,000 × g for

30 min at 4°C. Clarified lysates were cleaned by incubation with about 50 µl GSH-agarose and 25 µg GST per 2 × 10^6-cell-equivalent volume of lysate overnight at 4°C with inversion mixing. The beads were pelleted, and the supernatant, a clarified and clean lysate, was stored for the assay at -20°C.

A volume of well agitated slurry containing 10 µg of immobilized GST or an equimolar equivalent of immobilized GST-SH2(Lck) was transferred to a microfuge tube. Also transferred to each tube was about 100 µl of unadhered packed GSH-agarose beads as carrier beads (to offset the loss of beads during subsequent washes). Beads were mixed and pelleted, and the supernatant discarded.

Two hundred µl of cell lysate (2 × 10^6-cell-equivalent volume) were applied to the immobilized GST proteins and incubated 2 h at 4°C with inversion mixing. After 2 h, the beads were pelleted and washed 4 times in GLAB buffer with the phosphatase inhibitor cocktail. Careful attention was paid to removing as much of the supernatant of each wash as possible without inadvertently discarding beads and the adhered precipitate of interest. After washes, 100 µl of GLAB buffer were left on the resin for SDS-PAGE.

2.12 INFECTION OF ADHERENT CELLS

The lysis buffer used to prepare infected Vero, HEL, and HeLa cell lysate for immunoblot analysis was 1% Nonidet P-40, 0.25% sodium deoxycholate, 150 mM NaCl, 1 mM EGTA, 10 mM NaF, 10 mM β-glycerophosphate, 1 mM Na_3VO_4, 50 mM Tris-HCl (pH 7.4).

Vero, HEL, and HeLa cells were cultured to confluence in 6-well plates and infected at an MOI of 10 PFU/cell in serum-free culture medium for 1 h at 37°C, humidified. Serum-free culture medium was aspirated and discarded at 1 hpi, and FBS-containing culture medium was added for the remainder of each infection. Cell were harvested by first ensuring cells

were in suspension via scraping or vigourous pipette aspiration and dispensing. Cells were transferred microfuge tubes and pelleted at 4°C with 700 × *g*. Supernatant was discarded and 100 µl lysis buffer was applied to cells. Cells were vortexed in the lysis buffer and incubated on ice for 30 minutes. Cell debris was cleared by centrifugation at 15,000 × *g* for 15 min before storage at -20°C.

2.13 SDS-PAGE

Where indicated, cell lysates, pull-down precipitates, or other protein samples were resolved by SDS-PAGE. Polyacrylamide stacking gels were prepared as per the amounts and proportions outlined in *Molecular Cloning: a laboratory manual* (Sambrook and Russell, 2001). Protein samples were prepared for SDS-PAGE by mixing with 6X SDS lysis buffer (350 mM Tris pH 6.8, 30% glycerol, 10% SDS, about 1 mg/ml bromophenol blue) added 1:5 and incubation at 95°C for 5 minutes. A current with a voltage of between 100 and 150 V was applied to the gel until resolution of proteins of interest.

2.14 PONCEAU AND IMMUNOBLOT ANALYSES

Cell extracts were collected and cleared of debris as described for samples. Cell lysates or pull-downs were resolved by SDS-PAGE and transferred to a Amersham Hybond ECL nitrocellulose membrane (GE Healthcare Life Sciences). When analyzing VP11/12-GFP, a relatively high molecular weight (MW) protein, gels were transferred by applying 120 V, for 30 min, and then 80 V for 30 min. Otherwise, 100 V for 1 h were used to transfer proteins from gel to membrane. Where indicated, membranes were stained with Ponceau S and analyzed for visibility of abundant proteins. Membranes were blocked at 4°C with a non-specific binding reagent (Table 2-3) in Tris-buffered saline with Tween (TBS-T; 25 mM Tris pH 8, 150 mM NaCl, 0.1% Tween 20) for at least 1 h before incubation with

primary antibody (Table 2-3) at 4°C for 2 h or overnight. Membranes were washed in TBS-T 3 times before application of secondary antibodies. Primary antibody adherence was then detected by chemiluminescence using horseradish peroxidase-conjugated secondary antibodies (Table 2-4) and ECL Plus Western Blotting Detection Reagents (GE Healthcare Life Sciences). Alternatively, primary antibodies were detected by incubating the membrane with fluorochrome-conjugated secondary antibodies (Table 2-4) for at least 1 h at 4°C before scanning the membrane with an Odyssey infrared imaging system (LI-COR Biosciences, Lincoln, NE, USA) and, when indicated, quantitating fluorescence intensity using Odyssey 1.2 software. Blots were washed 3 times in TBS-T before detection of secondary antibodies.

Table 2-3. Primary antibodies.

Antibody (Dilution)	Source	Blocking Conditions	Manufacturer and Catalog No. (if applicable)
α-GST (1:20,000)	rabbit	5% milk	Abcam ab9085
α-GFP (1:30,000)	rabbit	1% BSA	Invitrogen A6455
α-Lck (1:10,000)	mouse (3A5)	1% BSA	Santa Cruz Biotechnology sc-433
α-pAkt(S473) (1:5,000)	rabbit	50% OBB	Cell Signaling #9271
α-Akt (1:5,000)	rabbit	50% OBB	Cell Signaling #9272
α-β-actin (1:30,000)	mouse (AC-15)	50% OBB	Sigma A5441
α-pTyr (1:5,000)	mouse (4G10)	50% OBB	Upstate 05-321X
α-VP16 (1:32,000)	mouse (LP1)	50% OBB	Minson*
α-UL46 (1:30,000)	rabbit	50% OBB	Nishiyama†

*A gift from Dr. Tony Minson (University of Cambridge, Cambridge, UK). †Given to the lab by Dr. Yukihiro Nishiyama (Nagoya University, Nagoya City, Aichi Prefecture, Japan) and referred to in Chapter 4 as α-VP11/12. 'OBB' is Odyssey Blocking Buffer (LI-COR Biosciences).

Table 2-4. Secondary antibodies.

Antibody (Dilution)	Source	Manufacturer	Detection
α-mouseIgG IRDye 800 (1:15,000)	donkey	Rockland	IR fluorescence
α-rabbitIgG Alexa Fluor 680 (1:15,000)	goat	Invitrogen	IR fluorescence
α-rabbitIgG HRP (1:30,000)	goat	Promega	chemiluminescence
α-mouseIgG HRP (1:30,000)	goat	Promega	chemiluminescence

2.15 AGAROSE GEL ELECTROPHORESIS

DNA was electrophoretically resolved in agarose gels. Agarose gels were prepared by dissolving 1% (w/v) agarose in Tris-acetate-EDTA (TAE) buffer (40 mM Tris, 20 mM acetic acid, 1 mM EDTA pH 8.0) under microwave heating and periodic agitation. Following gradual cooling of the solution to a touchable but hot temperature, ethidium bromide was added to the solution that was then agitated to allow even diffusion of ethidium throughout. The gel was then decanted into a cast with an appropriate comb and allowed to cool at room temperature to set with the required number of uniform wells. The cast with solidified gel was inserted into its associated tank and submerged in TAE buffer. Samples were electrophoretically resolved by applying current with voltage that did not exceed 8 V/cm.

2.16 RECOMBINATION-MEDIATED GENETIC ENGINEERING

2.16.1 Generation of *galK* cassette

The *galK* gene was amplified from pgalK using primers JRS599 and JRS600 (Table 2-2; Figure 4-2). These primers have pgalK-annealing sequence at their 3' termini and 50-nucleotide KOS-37 US3 homology arms as their 5' termini, designed to produce an amplicon with 50-basepair US3-homologous termini. This US3-homology design targets subsequent recombination of the amplicon to the R7041-deletion flanks in KOS-37, emulating the R7041 deletion in KOS-37. I, hereinafter, refer to recombination at these deletion-flanking loci as the *targeted recombination* events and the region between these loci as the *insertion-deletion locus*.

PCRs here and elsewhere were performed using Invitrogen Platinum

Pfx DNA Polymerase kit. Reagents from the kit and cycling parameters were in accordance with the manufacturer's recommendations, except $MgSO_4$ was used at a final concentration of 2 mM instead of the recommended 1 mM.

Following resolution by agarose gel electrophoresis, the amplicon was extracted using Qiagen Gel Extraction Kit according to the manufacturer's protocol.

2.16.1 Insertion of *galK*

As per the protocol described by Warming *et al.* (2005), SW102 was cultured, induced, and transformed with the *galK* cassette. A 15 ml liquid LB culture of SW102 KOS-37 or SW102 KOS-37ΔUL46 was grown at 32°C with 12.5 μg/ml chloramphenicol until OD_{600} reached between 0.55 and 0.60. The λ Red expression was then heat-induced at 42°C for 15 min and washed extensively in M9 salts (0.6% Na_2PO_4, 0.3% KH_2PO_4, 0.1% NH_4Cl, 0.05% NaCl). Pelleted SW102 were transformed with about 20 ng of the homology-flanked *galK* cassette in a 0.1 cm cuvette at 25 μF, 1.8 kV, and 200 Ω. Transformed SW102 were allowed to recover in liquid culture, washed extensively, plated on galactose-supplemented minimal medium, and incubated at 32°C until colonies were visible. Clones that persisted past initial selection, having yet to be convincingly verified as possessing the desired mutation, are hereinafter referred to as *candidate* clones or *candidate* recombinants.

2.16.2 Screening candidate clones for targeted recombination

Candidate *galK* clones were picked and streaked to single colonies on galactose-supplemented MacConkey agar to ensure a clonal pick and verify a *galK*$^+$ phenotype, as indicated by bright pink growth.

Colony PCRs were performed for further screening. Isolated MacConkey colonies were used to inoculate 5 ml LB cultures for glycerol

stock generation before inoculating PCRs. The first set of PCRs were performed with JRS3 and JRS4, *galK*-internal primers. Another set of PCRs was performed, priming cross the left targeted recombination site with JRS596 and JRS4. Analogous PCRs of the right junction with JRS3 and JRS597 were carried out. Finally, PCRs across the entire region from outside the targeted recombination sites, from non-targeted viral sequence on both sides, were performed to assay change in size of the entire region. These PCRs were performed with 1.5 mM $MgSO_4$ and at least 2X PCRx Enhancer Solution (Invitrogen), but otherwise in agreement with the Invitrogen protocol.

2.16.3 Excision of *galK* for desired US3 mutation

JRS611 and JRS612 (Table 2-2; Figure 4-7) are reverse-complementary 100-mer oligonucleotides, with 50 nucleotides of homology to both targeted recombination sites. JRS611 and JRS612 were hybridized by mixing 10 µg of each oligonucleotide in a volume of 100 µl 1X Invitrogen PCR buffer. The solution was heated to 95°C for 5 min and allowed to return to room temperature gradually. Ten µl of 3 M sodium acetate were added. DNA was precipitated by adding 250 µl 95% ethanol and cooling on ice for 10 min before pelleting at 30,000 × *g* for 10 min at 4°C. Supernatant was promptly removed and the DNA precipitate was washed once in 70% ethanol and air-dried. The pellet was dissolved in diH_2O.

SW102 KOS-37ΔUS3::*galK* or SW102 KOS-37ΔUL46ΔUS3::*galK* was grown to an OD_{600} of between 0.55 and 0.60 and heat-induced. Washed and pelleted, these SW102 were respectively transformed with JRS611-JRS612. After a 4 h recovery, the bacteria were washed extensively and plated onto DOG- and glycerol-supplemented minimal medium, and incubated at 32°C until colonies appeared.

Candidate recombinants were picked and streaked to single colonies on galactose- and chloramphenicol-supplemented MacConkey agar, ensuring a clonal pick and *galK*$^-$ phenotype, as indicated by yellow growth.

2.16.4 Generation of virus from US3-null BACmids

KOS-37ΔUS3 and KOS-37ΔUL46ΔUS3 BACmids were extracted from SW102 KOS-37ΔUS3 and SW102 KOS-37ΔUL46ΔUS3, respectively, using Qiagen Large-Construct Kit and associated protocol. BACmids were each transfected into 1×10^6 Cre-Vero cells using Invitrogen Lipofectamine 2000 as per the manufacturer's protocol. When total cytopathic effect was observed, transfected cells and medium were transferred to microfuge tubes, pelleted, and resuspended in serum-free medium. Cells were lysed in serum-free suspension by three freeze-thaws, and sonication in ice-cold water using a cup horn. Cell debris was cleared by centrifugation for 15 min at 15,000 × *g*, 4°C.

As the Cre-mediated recombination within Cre-Vero is presumably not perfectly efficient, the progeny were likely of heterogeneous genotype at their BAC locus, some virions still retaining the bacterial sequence in their genomes. As such, two rounds of plaque purification on Cre-Vero cells were undertaken to restrict viral populations to a homogenous genotype, one lacking the BAC, before stocks were grown.

Serial ten-fold dilutions of each virus solution were used to infect confluent Cre-Vero that were subsequently overlaid with 1% agarose with 1X DMEM, 5% FBS. These were incubated until plaques were visible, picked, and suspended in serum-free DMEM. This suspension was used to infect another 1×10^6 Cre-Vero cells to total cytopathic effect, which were harvested and subject to a second round of plaque purification.

2.16.5 Restoration of US3 in deletion BACmids for US3-repaired viruses

The *galK* gene was reinserted into US3 as per subsection 2.16.1. The construct used to excise *galK* and restore the wild-type sequence was the PCR amplicon of KOS-37 using primers JRS596 and JRS597. The resultant BACmids were transfected into Cre-Vero cells and also subject to two rounds of plaque purification.

Chapter III

Virion protein 11/12 binds Lck via the canonical SH2 binding mechanism

3.1 REFINING THE MODEL OF VP11/12-INDUCED SIGNALLING

Viruses have evolved means of commandeering cellular growth signalling for their own ends. This influence may create conditions favourable for the infection or extend cellular life, thus prolonging opportunity for viral replication. In examination of how HSV-1 tegument proteins may intersect growth signalling along the PI3K-Akt axis, Melany Wagner and Jim Smiley studied the post-translational modifications and interactions of VP11/12, as was described in Chapter 1.

Wagner and Smiley posited that VP11/12 is a viral analogue of an activated cellular growth receptor. VP11/12 could be using its phosphotyrosyl moiety YEEI to recruit and activate Lck (Wagner and Smiley, 2009). This tyrosine kinase would then phosphorylate other VP11/12 tyrosyl motifs, completing the binding site for PI3K regulatory subunit p85, YTHM (Wagner and Smiley, 2011), and a number of other signalling molecules. This would facilitate PI3K activation and consequent downstream Akt activation.

The purpose of the study described here was to test this model. Specifically, I aimed to elucidate how the first interaction, that between VP11/12 and Lck, may occur. These experiments and analyses establish the *in vitro* significance of the YEEI motif of VP11/12 in binding to the Src-homology 2 (SH2) domain of Lck via its canonical binding groove.

3.2 PREDICTED SH2 BINDING MOTIF IS WELL CONSERVED

To find potential binding motifs in the VP11/12's primary structure, Wagner and Smiley used MotifScan (ScanSite 2.0) to analyze the VP11/12

amino acid sequence. In doing so, they identified numerous binding motifs, which included YEEI (the putative Src-family kinase SH2 domain binding motif), YTHM (PI3K p85 SH2 domain), YENV (Grb2 SH2 domain), and NPLY (Shc PTB domain). To refine these results, the amino acid sequence was analyzed using both MotifScan and Eukaryotic Linear Motif search algorithms (Obenauer *et al.*, 2003; Puntervall *et al.*, 2003). Consensus hits between the two searches were visually screened against a multiple-sequence alignment of VP11/12 and orthologues from other herpesviruses. The hits were visually evaluated for conservation, as an indicator of functional relevance, and the four binding motifs mentioned above were well conserved (Figure 3-1). The optimal-affinity binding motif for SH2 domains of SFKs is Tyr-Glu-Glu-Ile (YEEI) (Songyang *et al.*, 1993). Among the six available sequences in the *Simplexvirus* genus (in GenBank), YEEI is completely conserved among five *Simplexvirus* species and well conserved in the sixth (Figure 3-1). Phospho-YEEI of VP11/12 is hypothesized to mediate the initiating interaction with Lck by binding its SH2 domain (Wagner and Smiley, 2009).

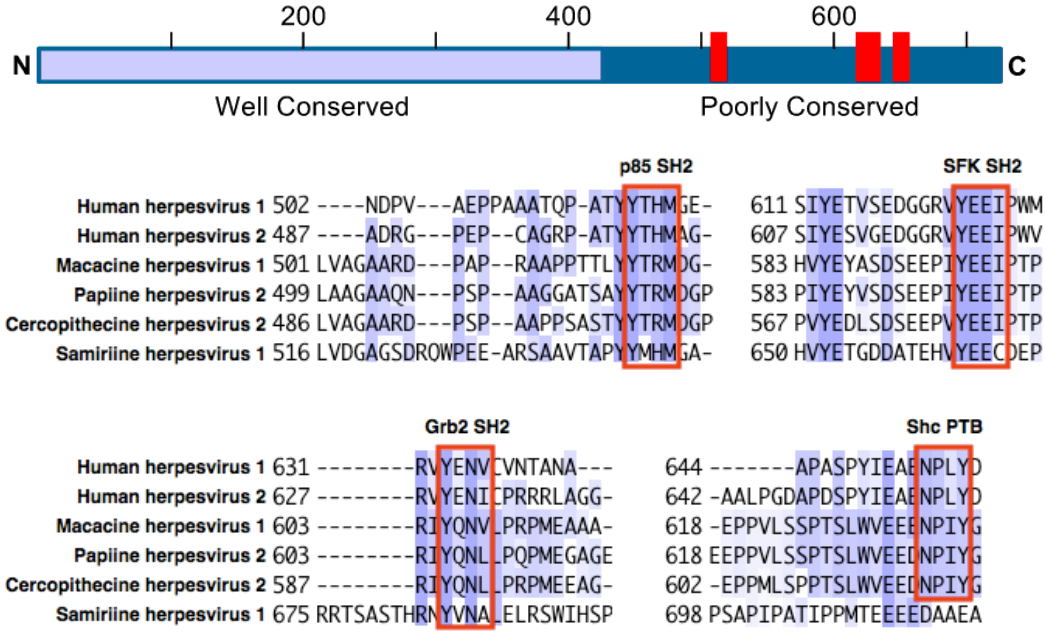

Figure 3-1. Conservation of putative binding motifs in carboxy terminus among VP11/12 orthologues of six *Simplexvirus* spp. Linear schematic of HSV-1 VP11/12 sequence is shown indicating the positions of the motifs (red) highlighted below and regions of general conservation or variability (top). Amino acid sequences from orthologues of the indicated viruses were aligned with MAFFT. Consensus hits from MotifScan and ELM were visually assessed for conservation on the alignment. Well conserved motifs and their predicted binding-partner domains are indicated (bottom). The images were generated using Jalview 2.5. The position of the first residue shown on each sequence in each panel is indicated.

3.3 GENERATING PURIFIED IMMOBILIZED AND SOLUBLE GST-SH2(LCK)

Previously, the lab procured a GST-fusion clone of the murine *Lck* SH2 domain to examine how this domain interacts with viral proteins. This construct allows us to assay the interactions of the SH2 domain itself. To that end, I sought to express the GST-SH2 fusion protein, and to purify and immobilize the protein on glutathione-agarose resin.

BL21 *E. coli* transformed with pGEX-SH2(LCK) or the empty vector pGEX were cultured in LB broth, and expression of GST-SH2(Lck) or GST, respectively, was induced with IPTG. The bacteria were lysed in GST Lysis and Binding Buffer (described in Chapter 2), which includes a nonionic detergent. Lysate produced from these induced bacteria was cleared by high-speed centrifugation and applied to glutathione-agarose beads. This resin was extensively washed and analyzed by Ponceau S stain, ensuring no impurities were observed and verifying a usable level of expression (Figure 3-2).

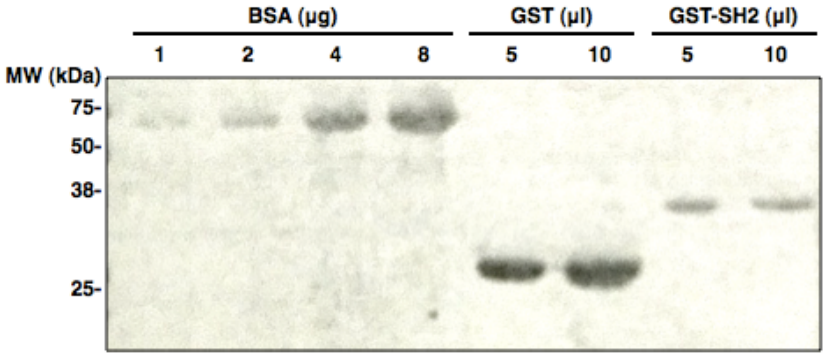

Figure 3-2. GST protein expression and purity. Suspensions of glutathione-agarose-immobilized GST and GST-SH2(Lck) were boiled in SDS lysis buffer for 5 minutes, resolved by 8% SDS-PAGE, and transferred onto a nitrocellulose membrane. The membrane was stained with Ponceau S. This was used to estimate protein concentration, evaluate purity, and test for degradation.

To produce soluble GST protein to facilitate reciprocal interaction assays, the proteins were eluted from the glutathione-agarose using GST Lysis and Binding (GLAB) Buffer supplemented with reduced glutathione. The solubilized protein was quantified by Bradford assay (Figure 3-3).

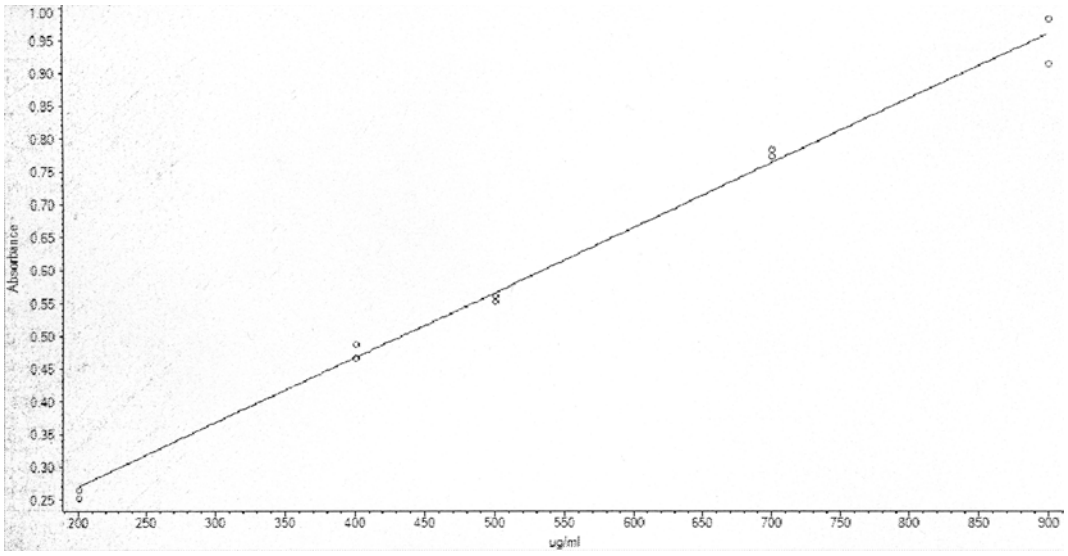

Figure 3-3. BSA standard curve used for soluble protein quantification. In this representative instance, bovine serum albumin solutions of known concentration in duplicate were reacted with Bio-Rad Protein Assay reagent as per the manufacturer's protocol and absorbance measured at 595 nm. Thermo Scientific NanoDrop 2000 software was used to plot the best fit line. Absorbance of GST-protein eluate dilutions were measured and concentration was solved as per best fit plot using the NanoDrop software.

3.4 THE LCK SH2 DOMAIN BINDS VP11/12

In view of a clearly predicted SH2 binding motif plainly conserved in

VP11/12, I tested the hypothesis that the VP11/12-Lck interaction can be mediated by the Lck SH2 domain using the GST-SH2(Lck) fusion protein. One million Jurkat T cells were mock-infected or infected at an MOI of 10 with: GHSV-UL46, a HSV-1 strain that encodes a carboxy-terminally GFP-tagged VP11/12; KOS-G, a strain that encodes GFP; or KOS, the wild-type strain from which GHSV-UL46 and KOS-G are derived. At 13 hours post-infection, these cells were harvested using GLAB Buffer. Lysates of these infected cells were incubated with agarose-immobilized Lck-derived GST-SH2, as well as GST as a control.

The precipitate was analyzed by immunoblot for GFP, VP16, and actin (Figure 3-4). In pull-downs using GST only, no proteins were detected. The abundant proteins, VP16 and actin, were not predicted to interact with GST-SH2(Lck) and were not pulled down from infections of any strain used. An α-GFP-reactive protein corresponding to the size of VP11/12-GFP was detectable on the GST-SH2(Lck) beads incubated with the GHSV-UL46 lysate. Given that the pull-down from the KOS-G infection did not contain GFP, and GST is unable to pull down GFP, the interaction of VP11/12-GFP and GST-SH2(Lck) was an SH2-VP11/12 interaction. The SH2 domain of Lck can co-precipitate VP11/12, while abundant cellular and viral proteins are not pulled down, suggesting that VP11/12 interacts with the SH2 domain of Lck.

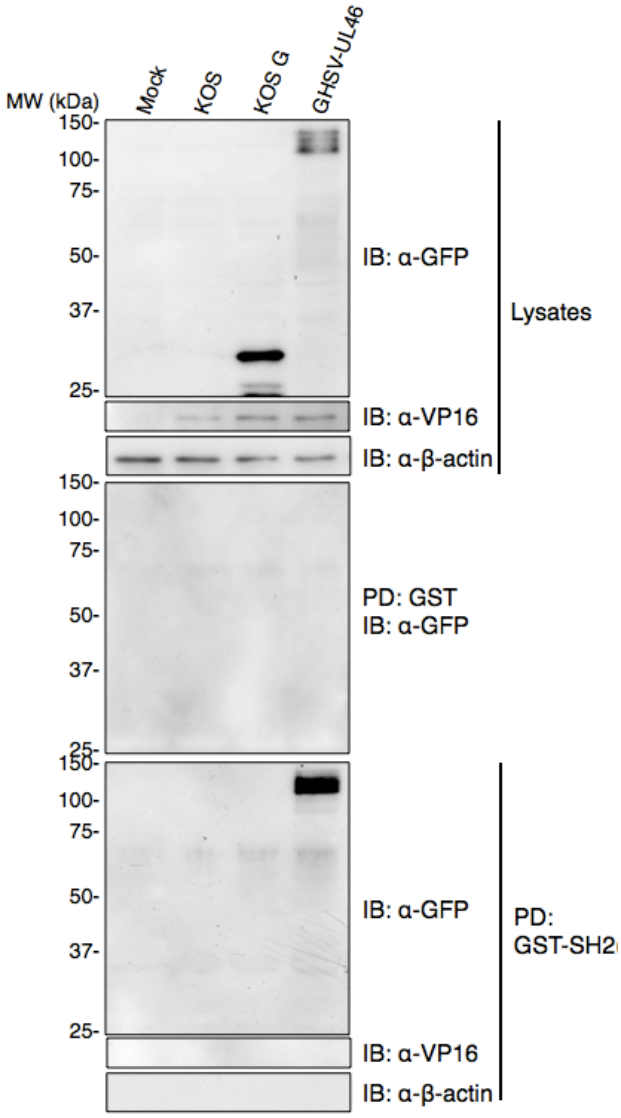

Figure 3-4. SH2 from Lck binds VP11/12. One million Jurkat T cells were infected at an MOI of 10 for 13 h and lysed in GLAB buffer. Lysates were incubated with resin-immobilized GST or GST-SH2(Lck) and the resultant pull-down was washed extensively. Each precipitate was boiled in SDS lysis buffer and resolved by 10% SDS-PAGE, transferred to nitrocellulose. Proteins were detected by immunoblot.

3.5 VP11/12 CAN DIRECTLY BIND THE LCK SH2 DOMAIN VIA THE CANONICAL MECHANISM

Based on the model proposed by Wagner and Smiley, a clear prediction is that this VP11/12-SH2 interaction is a direct association

mediated by the YEEI motif. If this is indeed that case, the established mechanism of SH2 binding applies: the YEEI-SH2 association is direct, with no intermediary molecules; the tyrosyl must be phosphorylated for binding to occur; reactivity is dependent on the residues carboxy-terminally adjacent to the phosphotyrosyl. Further, given the conformational regulation of Lck, this putative SH2 binding motif must out-compete the inhibitory phosphotyrosyl motif of Lck to adhere to SH2 and activate Lck.

Four synthetic dodecameric polypeptides were obtained to help address these hypotheses (Table 2-1). These peptides were amino-terminally biotinylated, allowing adherence to streptavidin-agarose resin and use as a molecular probe for interaction assays. The peptide sequences were derived from VP11/12 or Lck: (i) is a sequence from VP11/12 that includes the phosphorylated motif of interest (pYEEI); (ii) is identical to (i) except lacking any phosphoryl modification (YEEI); (iii) is a tyrosine-phosphorylated VP11/12 sequence that is not predicted to interact with Src-family kinase SH2 domains (pYTHM); and (iv) is the carboxy terminus of Lck which contains its phosphorylated SH2-inhibitory motif (pYQPQ).

The proposed model necessitates a hierarchy of SH2-domain reactivity among these peptides. If a phospho-YEEI moiety is indeed critical to initiate VP11/12-mediated signalling, the pYEEI peptide must have the greatest SH2 binding affinity, greater than the sequence-non-specific phosphotyrosyl peptide, pYTHM, and greater than the phosphorylated Lck carboxy terminus, pYQPQ. YEEI should be unreactive. Furthermore, these interactions must occur directly.

To test if the Lck SH2 domain can directly react with these peptides, I immobilized these peptides on agarose beads and incubated them with solutions of purified GST-SH2(Lck) or GST (Figure 3-5). The beads were washed extensively. Analysis of the resultant precipitate by immunoblot for

GST indicated the presence and relative quantity of any protein co-precipitated (Figure 3-6). From the relative quantity of SH2 co-precipitated, I infer the relative SH2 reactivity of each peptide.

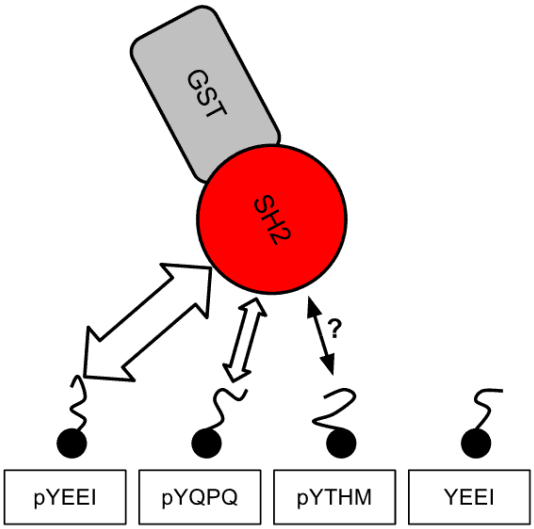

Figure 3-5. Illustration of hypothesized bead-immobilized peptide reactivity with Lck SH2. To be congruent with the VP11/12-induced signalling model, the pYEEI peptide must have the greatest reactivity with SH2, and YEEI is predicted to be unreactive.

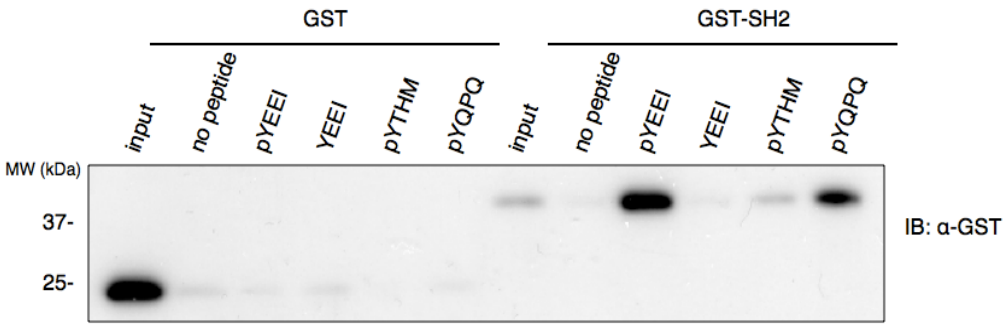

Figure 3-6. Peptide containing phospho-YEEI directly binds Lck SH2. Indicated peptides were immobilized on streptavidin-agarose beads and used to pull down from purified solutions of GST-SH2(Lck) or GST. Precipitates were boiled in SDS lysis buffer and resolved by 10% SDS-PAGE, transferred to nitrocellulose, proteins detected by immunoblot.

Marginal GST association with each peptide was detected, a background, non-specific association. Neither bare beads nor beads with adhered YEEI peptide were able to co-precipitate more GST-SH2(Lck) than background. In agreement with what is established of Lck regulation (see

subsection 1.3.2), pYQPQ co-precipitated GST-SH2(Lck) and was capable of direct binding. The pYEEI peptide also pulled down GST-SH2(Lck), suggesting that the VP11/12-SH2 interaction may be direct.

Congruent with the hypothesis, pYEEI pulled down the most GST-SH2(Lck) implying the greatest SH2-domain reactivity among the peptides. Surprisingly, pYTHM showed observable association with GST-SH2(Lck). Some replicates of this experiment showed pYTHM reactivity comparable to that of pYQPQ (data not shown). Consistently, however, pYTHM displays less capacity to pull down GST-SH2(Lck), weaker reactivity with SH2, than pYEEI. Agreeing with known factors affecting SH2-domain binding, YEEI did not precipitate any GST-SH2(Lck), indicating no SH2-domain reactivity.

These data indicate VP11/12-derived peptide containing the phospho-YEEI motif directly binds SH2 of Lck with greater affinity than a peptide of the Lck carboxy terminus. Moreover, the characteristics of this pYEEI-SH2 interaction conform to the established mechanism of SH2 binding, namely its dependence on tyrosyl phosphorylation and surrounding primary structure.

3.6 COMPETITIVE INHIBITION OF VP11/12-SH2 INTERACTION

The results of the preceding section showed that the pYEEI peptide (bearing the VP11/12 phospho-YEEI motif) binds directly to the SH2 domain of Lck. To determine if this interaction is necessary for the ability of Lck SH2 domain to pull down VP11/12 from infected-cell extract, I performed peptide competition assays (Figure 3-7). The prior GST pull-down experiment was performed in the presence of various concentrations of pYEEI or YEEI peptide (Figure 3-8). Ponceau analysis verified consistent levels of probe GST protein. The pYEEI titration showed a concentration-dependent inhibition of VP11/12-SH2 association, each

progressing concentration increase offsetting further amounts of pull-down protein. In contrast, YEEI has no competitive-inhibitory activity, as it was unable to prevent pull-down even at high concentrations. These observations are consistent with the idea that the phospho-YEEI motif mediates SH2 binding and the canonical SH2 binding groove is an important mediator.

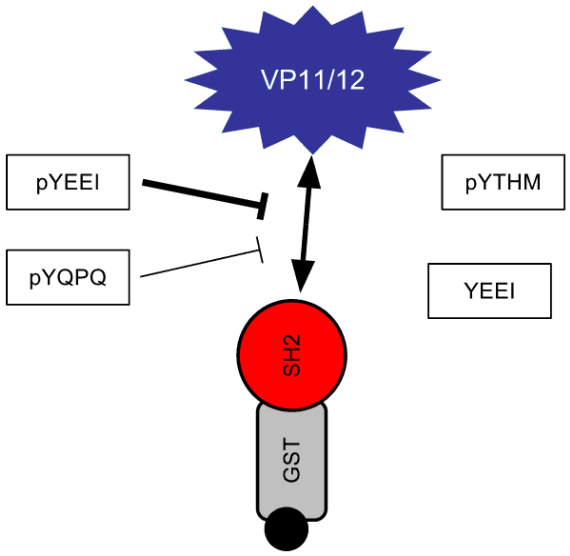

Figure 3-7. Illustration of hypothesized soluble peptide reactivity with Lck SH2 as indicated by competitive inhibition of interaction with VP11/12. To be congruent with the VP11/12-induced signalling model, the pYEEI peptide must have the greatest reactivity with SH2, and YEEI is predicted to be unreactive.

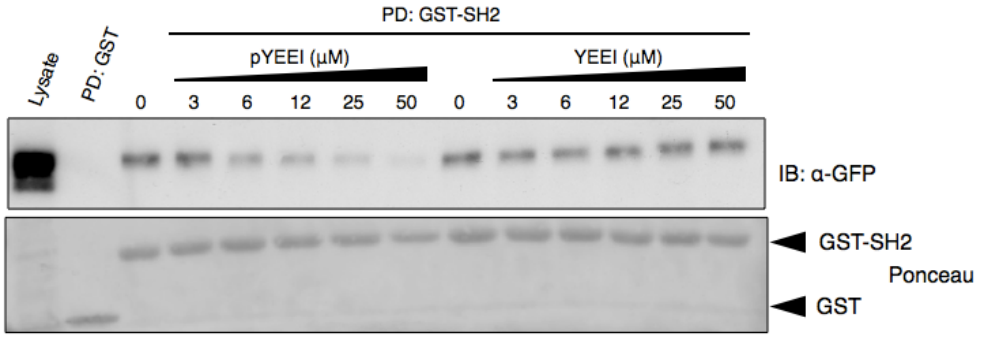

Figure 3-8. Increasing concentrations of pYEEI peptide competitively inhibits SH2-VP11/12 binding. Jurkat cells were infected with GHSV-UL46 and harvested 13 hpi in

GST lysis buffer. Clarified lysate was probed with GST-SH2 in the presence of indicated concentrations of indicated peptide and resultant pull-downs were resolved by 8% SDS-PAGE and transferred to nitrocellulose. Proteins were detected by Ponceau S staining and immunoblot.

Comparing pYEEI to pYTHM by the same methodology (Figure 3-9), pYEEI showed greater competitive inhibition of binding than the sequence-non-specific comparator reagent. At higher-range concentrations of either peptide, the interaction did not occur with pYEEI but still was observed with pYTHM. This result presents further congruence with the phospho-YEEI-SH2 interaction hypothesis.

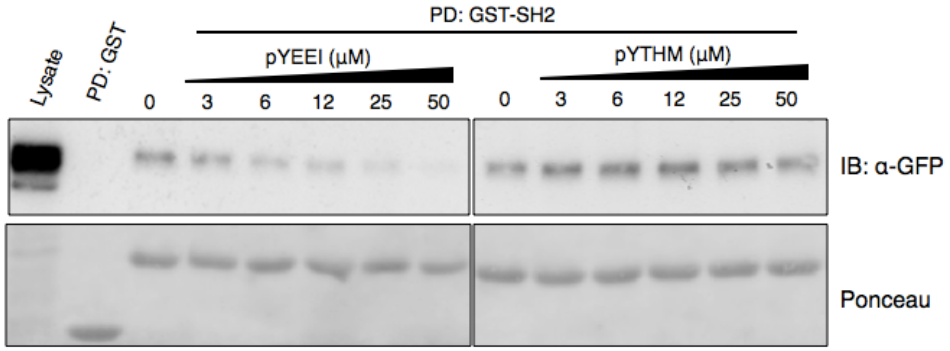

Figure 3-9. Competitive inhibition by peptide titration is a sequence-specific effect. Jurkat cells were infected with GHSV-UL46 and harvested 13 hpi in GST lysis buffer. Clarified lysate was incubated with GST-SH2(Lck) beads in the presence of indicated concentrations of indicated peptide and resultant pull-downs were resolved by 8% SDS-PAGE and transferred to nitrocellulose. Proteins were detected by Ponceau S staining and immunoblot.

3.7 COMPARING REACTIVITY OF YEEI AND THE LCK INHIBITORY MOTIF

In order for the hypothesized interaction between VP11/12 and the Lck SH2 domain to occur, phospho-YEEI must have greater SH2 affinity than the Lck inhibitory motif. This is an especially relevant consideration given this inhibitory motif is tethered to the SH2 domain, as both are constituents of full-length Lck. It follows that the pYEEI reagent should be able to co-precipitate full-length Lck despite the presence of a likely phosphorylated

inhibitory motif tethered to the interacting SH2 domain. This should occur in the absence of all other viral proteins.

Each of the four polypeptide reagents were used to probe uninfected-Jurkat cell lysate. These peptides were each bound to streptavidin-agarose beads and incubated with the lysate. After extensive washing, the bead-associated protein was analyzed by α-Lck immunoblot (Figure 3-10). Pull-down using control peptides revealed notable, but consistent, levels of background Lck. Importantly, pYEEI showed the greatest Lck affinity, even greater than that of pYQPQ, with Lck-derived inhibitory sequence. This observation agrees with the previous peptide pull-down that showed pYEEI reactivity exceeding that of pYQPQ (Figure 3-6). Likewise, a comparative peptide competition assay with these two reagents further supports this idea (Figure 3-11). This is evidence that the proposed VP11/12 SH2 binding motif can override Lck-endogenous SH2 inhibitory binding.

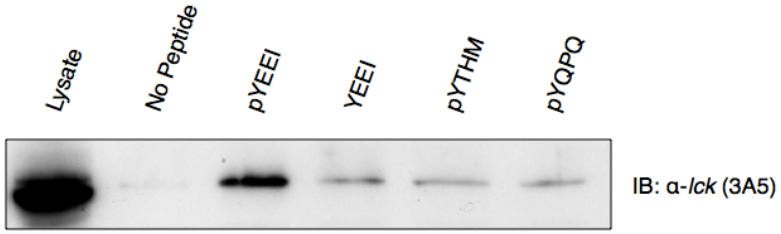

Figure 3-10. Phospho-YEEI peptide pulls down endogenous full-length Lck. Thirty million Jurkat cells were lysed in GLAB buffer. Clarified lysate was probed with indicated immobilized peptide and resultant pull-downs were resolved by 10% SDS-PAGE, transferred to nitrocellulose, and subjected to immunoblot analysis.

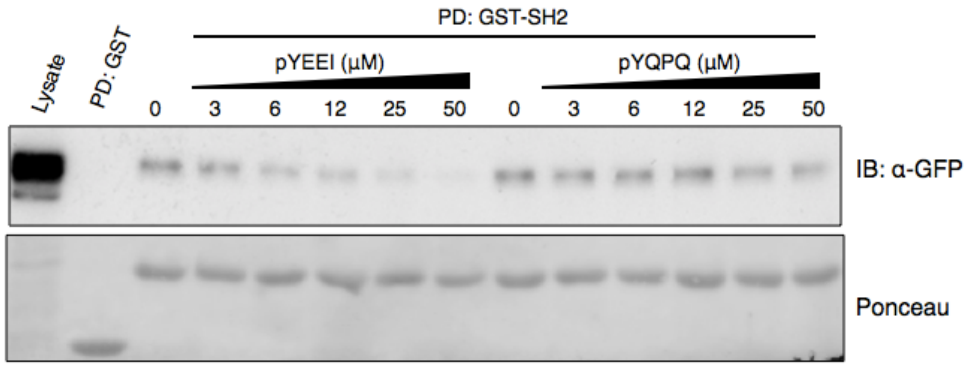

Figure 3-11. Peptide pYEEI shows greater affinity to Lck SH2 than Lck-derived inhibitory sequence. Jurkat cells were infected with GHSV-UL46 and harvested 13 hpi in GST lysis buffer. Clarified lysate was probed with GST-SH2 in the presence of indicated concentrations of indicated peptide and resultant pull-downs were resolved by 8% SDS-PAGE and transferred to nitrocellulose. Proteins were detected by Ponceau S staining and immunoblot.

3.8 SUMMARY

The experiments described here test the validity of the VP11/12-induced signalling model. In examination of how VP11/12 recruits and activates Lck, a possible mechanism of this proposed signal-initiating interaction was characterized *in vitro*. *In silico* analysis revealed that a predicted optimal-affinity Src-family kinase SH2 binding motif is well conserved among simplexviruses. A VP11/12-derived peptide containing this motif bound the SH2 domain of Lck in a manner consistent with canonical SH2 interactions. This VP11/12 peptide was further capable of out-competing the inhibitory motif from Lck itself. The evidence suggests that VP11/12 may commandeer and activate Lck by interacting with its SH2 domain via the YEEI motif.

Chapter IV

Generation of US3PK knock-outs by targeted deletion in the unique-short 3 open reading frame from the KOS-37 BACmid

4.1 REGULATION OF VP11/12 BY US3PK

In delineating the function of HSV-1 VP11/12, the lab is also investigating factors that affect its regulation. Accordingly, US3PK is of interest for its reported phosphorylation of VP11/12 (Matsuzaki *et al.*, 2005). Taken with further observations from prior studies, however, US3PK has seemingly antagonistic roles.

Wagner and Smiley (2011) reported that VP11/12 activates Akt. A study by the Nishiyama group on HSV-2 orthologues showed that US3PK phosphorylates VP11/12; the stability of VP11/12 is dependent on US3PK as more rapid degradation of VP11/12 is observed during infection with US3PK-null mutants (Matsuzaki *et al.*, 2005). Interestingly, the Roizman group established that US3PK inhibits Akt activation (Benetti and Roizman, 2006).

Though US3PK is a likely VP11/12 modulator, this apparent contradiction—an inhibitor of Akt that may stabilize an activator of Akt—raises issues concerning the function of US3PK-VP11/12 interaction. It is unclear whether US3PK regulates the stability of VP11/12 in HSV-1 and, if so, whether US3PK inhibits Akt through its action on VP11/12. The effect on Akt phosphorylation of removing both VP11/12 and US3PK is unknown. Any experiment to clarify these uncertainties requires viral mutants, knock-outs of either gene and a double knock-out of both. Further, to control for inter-strain genomic variation, the desired mutants must be generated from the same strain.

Though US3- and UL46-null single mutants have been generated

previously, they are not of a shared parental strain. The Roizman group has generated a US3-null mutant from strain F and its corresponding rescue mutant, respectively designated R7041 and R7306, and uses these extensively in its study of US3PK. For previous studies in the lab, Wagner generated a UL46 deletion mutant from strain KOS-37, along with its rescue mutant (Zahariadis *et al.*, 2008).

To develop reagents for addressing uncertainties in the function of US3PK, I generated the remainder of the mutants from a KOS-37 genomic background: a US3 knock-out from KOS-37 and its rescue; and a double knock-out of both UL46 and US3 from Wagner's UL46-null KOS-37 and its US3 rescue.

4.2 US3PK INHIBITS AKT ACTIVATION IN MULTIPLE CELL LINES

The Roizman group showed that US3PK was responsible for Akt inhibition in HEp-2 cells (Benetti and Roizman, 2006). To verify and test the cell-type dependence of this finding, I replicated this experiment in Vero and HEL cells. One million Vero or HEL cells were infected with the R7041 US3 mutant in parallel with R7306 US3 repair, wild-type strain F, and mock infection. The cells were harvested at 4 hpi. Infected-cell lysates were analyzed by immunoblot, probing for phospho-Akt, total Akt, and actin as a loading control (Figure 4-1). Actin levels indicated similar loading among lanes. Phospho-Akt levels indicate the proportion of Akt activated as total Akt is fairly constant.

In both cell lines, without US3PK there was more activated Akt detected, and when US3PK was present a lesser proportion of Akt was activated. In agreement with Roizman and colleagues, these observations suggest US3PK indeed inhibits Akt activation.

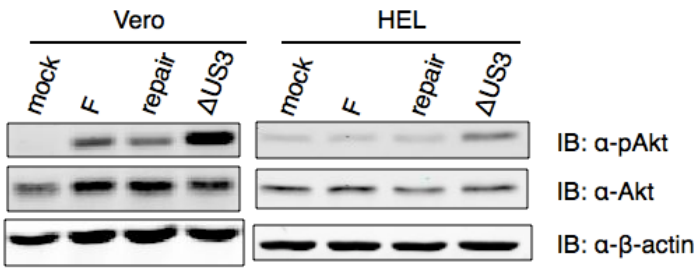

Figure 4-1. Virus-induced Akt phosphorylation is potentiated in the absence of US3. One million Vero cells or human embryonic lung (HEL) fibroblasts were infected with the indicated viruses and lysed at 4 hpi. Lysates were resolved by 10% SDS-PAGE, transferred to nitrocellulose, and subjected to immunoblot analysis using infrared imaging.

4.3 DEVISING AN EXCISION STRATEGY AT THE US3 LOCUS

In planning a deletion from the HSV-1 genome, several complicating factors are at play. Transcripts overlap in both directions, sometimes starting within the open reading frame (ORF) of another gene. Undoubtedly, transcriptional-regulatory elements of a given gene could be found within adjacent genes. In regions where such overlap is apparent, careful consideration is critical for achieving the required phenotype while avoiding unintended effects on the expression of neighbouring genes.

Wagner's mutation at UL46 was a seamless, complete deletion of its open reading frame (Zahariadis *et al.*, 2008). A mutation deleting the entire US3 ORF was not performed because such a mutation would remove the transcription initiation codon of US2 and cut close to the start of US4. Therefore, I opted instead to emulate the partial US3 deletion in R7041 (Purves *et al.*, 1987), the strain F-derived US3-null mutant, as this was already accepted in the literature as a suitable US3 knock-out deletion (Purves *et al.*, 1991; Purves *et al.*, 1992; Leopardi *et al.*, 1997; Munger *et al.*, 2001; Benetti and Roizman, 2004; Liu *et al.*, 2007; Peri *et al.*, 2008).

4.4 THE RECOMBINEERING TACTIC

KOS-37 is the designation of the BACmid encoding HSV-1 wild-type

strain KOS genome with floxed BAC elements in the UL37-UL38 intergenic region. Upon transfection into permissive cells, this BACmid is infectious, producing replication-competent virus. The floxed BAC vector can be excised from the viral genome by plaque purification in permissive Cre-expressing cells, leaving only a single *loxP* element.

Recombination-mediated genetic engineering, or recombineering, allows for the manipulation of BACmids using homologous DNA recombination. This was the technique used by Wagner to generate the UL46 knock-out from KOS-37 (Zahariadis *et al.*, 2008). As described by Warming *et al.*, the technique requires the transformation of a linear dsDNA recombination substrate with homology-targeted flanks and DNA recombination machinery capable of efficiently using very short regions of homology, such as that encoded by λ phage (Warming *et al.*, 2005).

The *E. coli* strain SW102 was constructed specifically to allow recombineering using *galK* as a selection marker with two crucial features: *galK*-deficiency and an inducible defective λ prophage. SW102 expresses λ Red recombination genes: *exo*, encoding a 5'-3' exonuclease to generate 3' overhangs on the substrate; *bet*, a single-stranded binding protein that mediates strand invasion of overhangs into homologous (target) sequence; and *gam*, an inhibitor to prevent degradation of the transformed construct by *E. coli*-endogenous linear-dsDNA exonuclease RecBCD. Expressed from a stably integrated replication-incompetent prophage in the SW102 chromosome, these genes are controlled by a temperature-sensitive repressor. Heat induces expression of this system, allowing action upon the homologous flanks of the transformed linear dsDNA and consequent integration into the BACmid. Given the SW102 *galK* deficiency, the *galK* gene is a useful BACmid selection marker because one may select both for and against its presence. One can generate a marker-free mutation using a two-step protocol that: (i) produces a $galK^+$ intermediate BACmid, selecting

for *galK*; and (ii) removes *galK* in second recombination reaction, selecting then against *galK*.

In step (i), using SW102 a *galK* cassette flanked by BACmid-homologous arms targets the recombination to the desired BACmid locus, inserting *galK*. Encoding bacterial galactokinase, *galK* is necessary for a bacterium's metabolism of galactose. SW102's *galK*$^-$ phenotype can be complemented *in trans* by a *galK*$^+$ BACmid. Selection for *galK* presence is achieved by growth on a medium that supplies galactose as the sole carbon source, strongly favouring the *galK*$^+$ from SW102 cultures of otherwise heterogeneous *galK* phenotype.

Step (ii) removes *galK* in a second targeted recombination. A carefully constructed linear dsDNA with *galK*-flanking homology is transformed into heat-induced SW102, excising *galK* from the BACmid, integrating the linear construct in its place. Selection against *galK*$^+$ SW102 is performed by culture on medium that contains 2-deoxygalactose (DOG). DOG is phosphorylated by GalK to produce 2-deoxygalactose-1-phosphate, a toxic product that cannot be further metabolized, a build-up that kills affected cells. In theory, the resultant, surviving SW102 harbour the desired mutant BACmid, free of *galK*. The success of the protocol, however, hinges upon the planning and construction of the dsDNA reagents used.

4.5 INSERTION OF THE SELECTION MARKER IN US3

To generate the homology-flanked *galK* construct for the US3 deletion, *galK* was PCR-amplified from pgalK using primers JRS599 and JRS600 (Figure 4-2). The amplicon was resolved by agarose gel electrophoresis, excised, and purified.

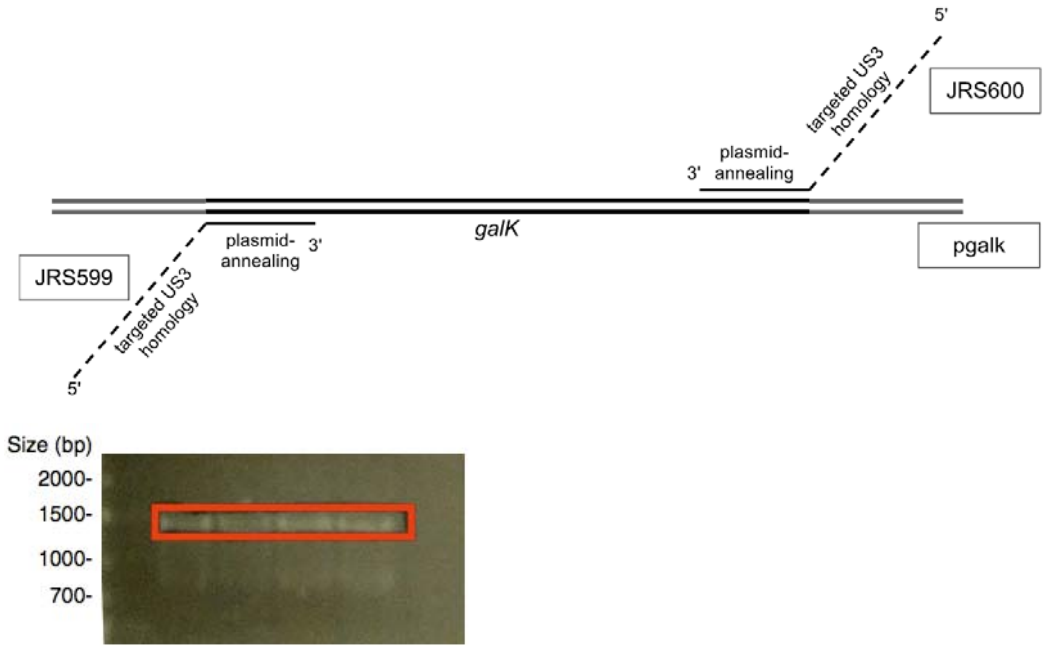

Figure 4-2. Generation of US3-targeted galK cassette by PCR. PCR primers were designed to generate a *galK*-containing amplicon with flanking US3 homology for subsequent targeted recombination (top). Dashed lines represent KOS-37 BACmid-derived sequence. This representation is not to scale. PCR products were resolved by 1% agarose gel electrophoresis, stained with ethidium bromide, and imaged while ultraviolet-transilluminated. In each of the 4 lanes of this representative amplification (bottom), the amplicon of pgalK with homology-tailed primers was resolved by 1% agarose gel electrophoresis, excised (red), and purified.

SW102 KOS-37 or SW102 KOS-37ΔUL46 were heat-induced, transformed with the *galK* cassette, and cultured on medium whose sole carbon source was galactose. Candidate *galK*$^+$ recombinants were screened by PCR (Figure 4-3), testing for the presence of *galK*, amplification across targeted recombination sites, and size change across the entire insertion-deletion locus (Table 4-1).

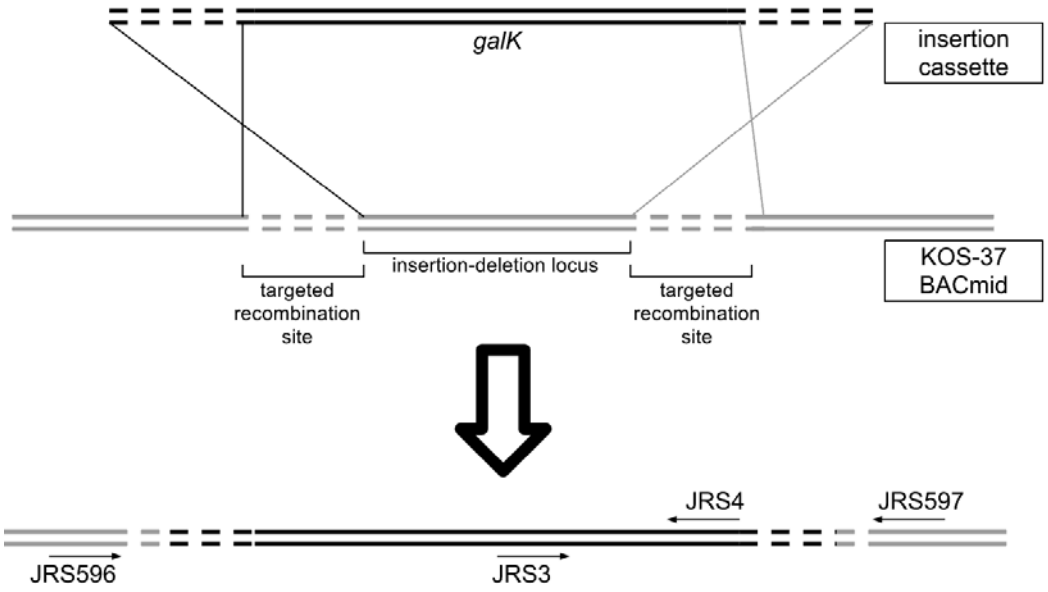

Figure 4-3. Illustration of targeted recombination and *galK*⁺ intermediate product. Induced recombination was designed to delete part of US3 and insert *galK* at the same locus. Approximate binding locations of primers used in screening are indicated. This is not to scale.

Table 4-1. Predicted PCR amplification products from parental, intermediate, and final BACmid templates given targeted recombination occurrence.

Template	Left Primer	Right Primer	Calculated Size (bp)
KOS-37	JRS596	JRS597	1546
KOS-37ΔUS3::*galK*	JRS3	JRS4	403
KOS-37ΔUS3::*galK*	JRS596	JRS4	1480
KOS-37ΔUS3::*galK*	JRS3	JRS597	840
KOS-37ΔUS3::*galK*	JRS596	JRS597	1917
KOS-37ΔUS3	JRS596	JRS597	686

Predictions pertaining to KOS-37 and its derivatives are also applicable to KOS-37ΔUL46 and its derivatives.

First, to test for the acquisition of *galK*, the candidate clones were PCR-amplified using *galK*-internal primers. Using primers JRS3 and JRS4 (Figure 4-3), internal *galK* amplification products indicated the presence of *galK* in all of the tested candidate KOS-37ΔUL46ΔUS3::*galK* and candidate KOS-37ΔUS3::*galK* recombinants (Figure 4-4). Amplification from pgalK was

performed as a positive control, and the apparent sizes of the products from the candidate recombinants matches that of the positive control.

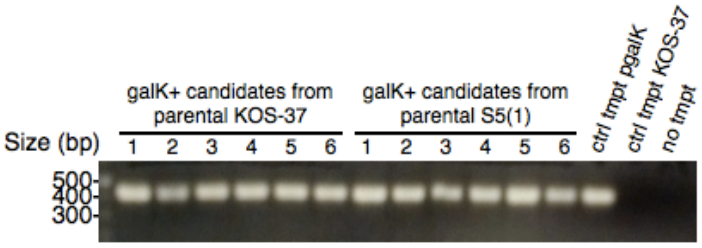

Figure 4-4. PCR screen for presence of *galK*. Candidate *galK*$^+$ recombinant BACmids were extracted, and each were subjected to PCR with primers JRS3 and JRS4, priming sequence internal to *galK* (Figure 4-3). PCR products were resolved by 1% agarose gel electrophoresis, stained with ethidium bromide, exposed to ultraviolet transillumination, and imaged. Amplification result from pgalK and parental KOS-37 templates, as well as no template, are shown at the far right. As per Melany Wagner's designation of the BACmid, KOS-37ΔUL46 is referred to here as 'S5(1)'.

A second PCR screen was an attempt to amplify via priming from bacterial to viral sequence, producing produce an amplicon if and, likely, only if the targeted recombination had indeed occurred. Candidate BACmid 2 from parental KOS-37 and candidate 2 from parental KOS-37ΔUL46 (Figure 4-4) were selected for this further screening. Priming from inside *galK* and from KOS-37 sequence outside the targeted recombination region, amplification across sites where the targeted recombination occurred would produce an amplification product of predicted size (Table 4-1). Thus, amplification across targeted recombination junctions was performed next to screen for BACmids that had undergone the targeted recombination, integrating *galK*. Attempted PCR from the parental KOS-37 BACmid produced no product, which was expected as *galK* sequence is not present in the BACmid or SW102 genome. One of each set (candidate 2 of both sets) of candidate recombinants that had shown *galK* acquisition at the first PCR screen was subjected to this second screen. Amplification products of PCRs

across the left junction with primers JRS3 and JRS596 are of expects size (Figures 4-3 and 4-5). So too are amplicons of PCRs across the right junction with primers JRS4 and JRS597 (Figures 4-3 and 4-5).[1]

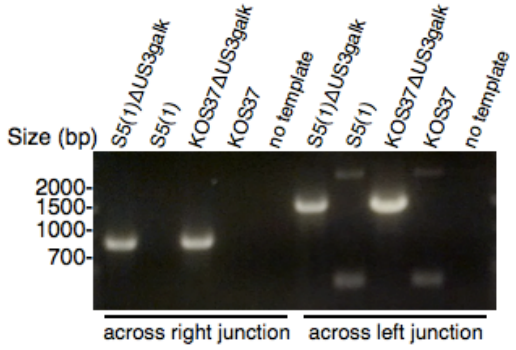

Figure 4-5. Screening for contiguous junctions of anticipated size at targeted recombination sites. Extracted BACmids were PCR-amplified across the left targeted recombination junction using primers JRS596 and JRS4 and across the right targeted recombination junction using primers JRS3 and JRS597 (Figure 4-3). PCR products were resolved by 1% agarose gel electrophoresis, stained with ethidium bromide, transilluminated with ultraviolet light, and imaged. The UL46-null KOS-37 BACmid is referred to here as 'S5(1)' in accordance with the designation used by Melany Wagner.

The third PCR screen was designed to test if the expected size change occurred at the insertion-deletion locus via an amplification across the entire insertion-deletion site from outside the recombination regions. The sizes of the resultant amplification products were compared to calculated sizes (Table 4-1), anticipated assuming the occurrence of the targeted recombination events (Figure 4-3). The PCR amplification product made using JRS596 and JRS597 primers showed the expected size difference in comparison with that of a parental BACmid template (Figure 4-6). A small, unanticipated amplification product was observed in PCRs that included JRS596, likely a consequence of non-specific annealing within US3. These data suggest that the target recombination events occurred, integrating *galK*

[1] I define 'left' and 'right' as per the HSV-1 genome orientation and configuration in GenBank, accession no. NC_001806.1. This is the orientation depicted in Figure 4-3.

into the respective BACmids at the desired locus.

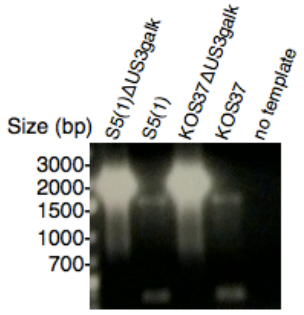

Figure 4-6. Verifying size change of the insertion-deletion locus and flanking targeted recombination regions. BACmid extracts were PCR-amplified using primers JRS596 and JRS597 (Figure 4-3). Amplification products were electrophoretically resolved in a 1% agarose gel, stained with ethidium bromide, UV-transilluminated, and imaged. 'S5(1)' is the KOS-37ΔUL46 BACmid.

4.6 REMOVING SELECTION MARKER TO PRODUCE SEAMLESS DELETION

To remove *galK* for a scarless US3 deletion, restoring the BACmid to its *galK*$^-$ phenotype, complementary oligonucleotides JRS611 and JRS612 were annealed, forming a linear dsDNA construct that models the insertion-deletion locus deleting *galK*. Composed of 100 basepairs, the JRS611-JRS612 hybrid was designed to possess 50 basepairs of homology to the left targeted recombination locus and 50 basepairs of homology to the right targeted recombination locus in the genomic orientation (Figure 4-7).

SW102 KOS-37ΔUS3::*galK* or SW102 KOS-37ΔUL46ΔUS3::*galK* was cultured, heat-induced, and transformed with the JRS611-JRS612 hybrid (Figure 4-2). These were screened by PCR with primers JRS596 and JRS597 across the insertion-deletion locus. Several candidate recombinants show the expected size at this locus (Figure 4-8). Given the GalK-deficient phenotype exhibited on MacConkey agar and that expected size change of the PCR product, these data suggest that these candidate recombinants

indeed have undergone targeted recombination with JRS611-JRS612. BACmid 6 from the ΔUS3 candidates and BACmid 4 from the ΔUL46ΔUS3 (Figure 4-8) were selected for virus generation and repair cloning.

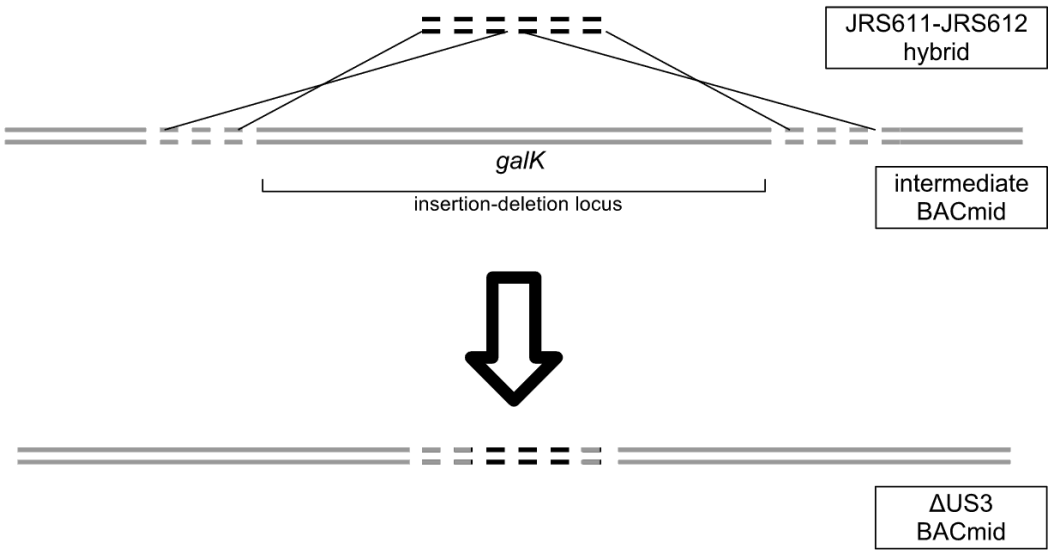

Figure 4-7. Illustration of targeted recombination for *galK* excision. Induced recombination with the JRS611-JRS612 dsDNA was targeted to delete *galK* from the BACmids. This representation is not to scale.

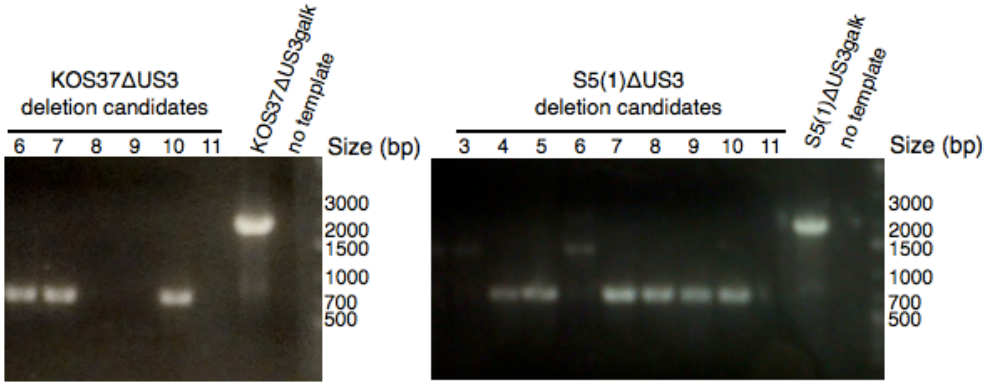

Figure 4-8. Screening candidate *galK*⁻ recombinants for anticipated size change. Candidate recombinant BACmids were PCR-amplified using JRS596 and JRS597. Products were resolved by 1% agarose gel electrophoresis, stained with ethidium bromide, and imaged with ultraviolet transillumination.

4.7 RESTORING US3

To ensure that any phenotypes observed in the US3 knock-outs were due to deletion of US3 rather than unintended effects of the cloning procedure, I next restored the US3 locus of KOS-37ΔUS3 and KOS-37ΔUL46ΔUS3. In creating the restored BACmid, an analogous protocol to that outlined in section 4.5 was employed. First, I introduced *galK* into the insertion-deletion locus by the targeted recombinations with the *galK* insertion cassette. Second, to remove *galK* and replace the excised US3 portion, the transformed reagent was instead a PCR product of the parental KOS-37 US3 locus produced with primers JRS596 and JRS597 (data not shown). Screening for size change in US3 for the intermediate and final BACmids (Figure 4-9), the locus changes in size as expected (Table 4-1).

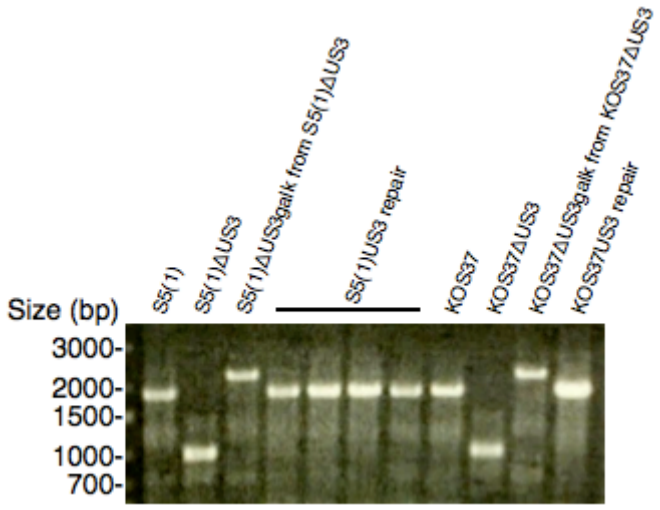

Figure 4-9. PCR amplification across insertion-deletion locus of parental, knock-out, restoration-intermediate, and US3-restored BACmids. BACmid extracts were each amplified using JRS596 and JRS597 primers. Products were resolved by 1% agarose gel electrophoresis, ethidium bromide-stained, and imaged with exposure to ultraviolet transillumination.

4.8 GENERATION OF VIRUS

The generated deletion and rescue BACmids were transfected into Cre-Vero cells, stably transfected with Cre recombinase, and incubated until plaques were visible. This virus was subjected to two rounds of plaque

purification. Prior to generation of US3-restored viruses, preliminary analyses were performed on the knock-out viruses and are described in the following sections.

4.9 ANALYSIS OF AKT ACTIVATION PHENOTYPE

As inferred via knock-out mutations, VP11/12 *activates* Akt (Wagner and Smiley, 2011), US3PK *inhibits* Akt (Benetti and Roizman, 2006), and HSV-2 orthologues of the proteins interact, US3PK phosphorylating and stabilizing VP11/12 (Matsuzaki *et al.*, 2005). A point of interest is the Akt activation phenotype of the UL46-US3 double knock-out that was as yet unknown.

Vero cells were infected with the double knock-out, infected with the single knock-outs, or mock-infected. Cell extracts from 4 hpi were electrophoretically resolved and analyzed by immunoblot for Akt activation. (Figure 4-10). In agreement with previous observations, virus-induced Akt activation was indeed inhibited in UL46-null infection and enhanced in US3-null infection. Infection in the absence of both genes produced an inhibited-activation Akt phenotype comparable to that of UL46-null infection. While this assay is not well controlled, lacking detection of *total* Akt levels, this observation agrees with more extensive characterization of this virus performed by labmate Kevin Quach (Quach and Smiley, unpublished data). This implies that VP11/12 is the upstream modulator of Akt. It is further implied that the action of US3PK to inhibit Akt is subordinate, and possibly subsequent, to VP11/12-induced Akt activation.

It remains unclear as to whether US3-induced Akt inhibition arises from US3PK action on VP11/12 directly or its interaction with any other factor. If US3PK veritably stabilizes VP11/12 in HSV-1 infection as is the case with HSV-2, US3PK likely inhibits Akt through one or more of its wide array of interacting partners and not via its phosphorylation of VP11/12.

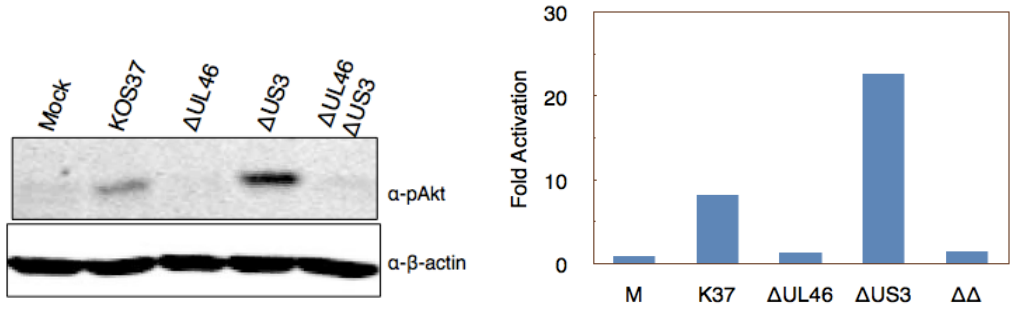

Figure 4-10. Virus-induced Akt activation is inhibited during double knockout infection. One million Vero cells were infected with the indicated viruses and lysed at 4 hpi. Lysates were resolved by 10% SDS-PAGE, transferred to nitrocellulose, and subjected to immunoblot analysis using infrared imaging (left). Detection of phospho-Akt was quantitated and normalized to actin levels (right).

4.10 VP11/12 EXPRESSION IN US3PK-DEFICIENT INFECTION

The Nishiyama group previously examined VP11/12 in HSV-2 infection with or without US3PK (Matsuzaki *et al.*, 2005). They observed that in US3-null infection apparent VP11/12 expression was notably decreased compared to wild-type infection. Their US3PK-deficient infections of Vero cells showed the appearance of α-VP11/12-reactive species of slightly greater and lesser electrophoretic mobility, while some wild-type infection VP11/12 species were not detected. As the Nishiyama group was examining close HSV-2 orthologues, one would expect HSV-1 VP11/12 and US3PK to have a congruent relationship. The newly generated HSV-1 US3-null mutants allowed the examination of whether these observations would hold true in HSV-1 KOS-37 infection.

One million Vero cells were infected with the UL46 mutant, US3 mutant, or the double knock-out, in parallel with mock and KOS-37 infection. At 8 or 12 hpi, cells were harvested and subject to immunoblot analysis. The nitrocellulose membrane was probed for actin, VP16, and VP11/12 (Figure 4-11). Actin levels, a loading control, verified a comparable number of cells used between samples. VP16 was an infection control, and levels ensured that a similar quantity of virus was used for infection. VP11/12

was detected in KOS-37 and US3-null infection at both time points. VP11/12 was not observed in mock, UL46-null, or double knock-out infections, as would be expected.

KOS-37 infections produced two VP11/12 species of slightly different mobility; the lower, more mobile species was the more abundant while the higher, less mobile species was only barely detected. In US3PK-deficient infections, conversely, additional VP11/12 species of lesser, but not greater, electrophoretic mobility were observed in addition to those observed in KOS-37 infection. These are not congruent with the electrophoretic mobility species reported by Matsuzaki *et al.* (2005).

Apparent VP11/12 levels were quantitated (Figure 4-11). At 8 hpi, a two-fold decrease of VP11/12 was detected in US3PK-deficient infection relative to KOS-37 infection. At 12 hpi, a two-fold enhancement of VP11/12 levels were observed compared to wild-type infection. A decreased detection of VP11/12 in US3-null infection, as observed at 8 hpi, agrees with the Matsuzaki *et al.* (2005) report of the HSV-2 orthologues. VP11/12 abundance that is enhanced in US3-null infection at 12 hpi directly contradicts the expectation, given that HSV-2 VP11/12 levels are severely diminished when HSV-2 US3PK is knocked out at the same time post-infection.

These data suggest that expression and/or degradation levels of HSV-1 VP11/12 as they relate to US3PK expression are not the same as observed in HSV-2. Further, the post-translational modification, as indicated by electrophoretic mobility, of VP11/12 does not change with the same pattern when US3 is removed.

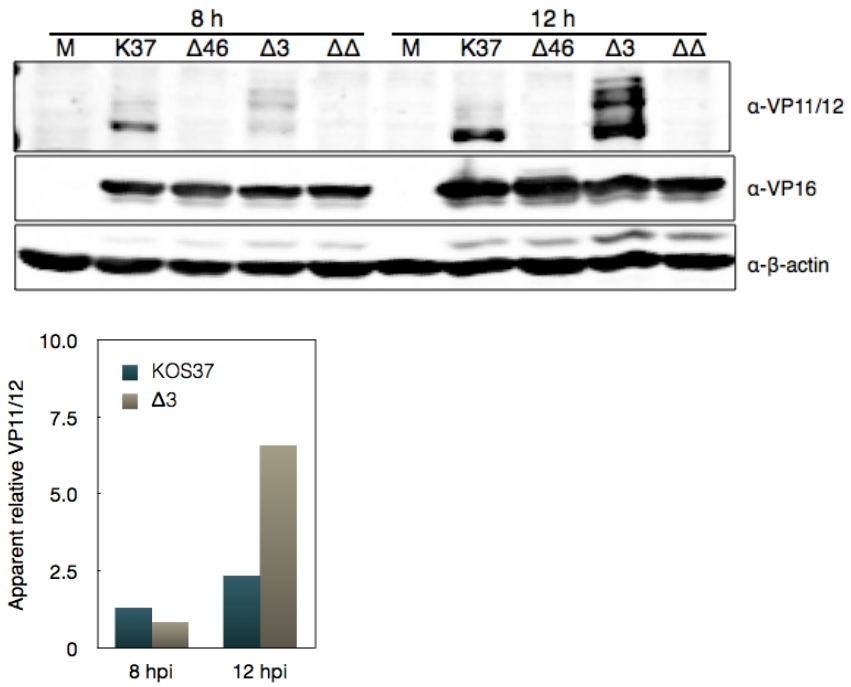

Figure 4-11. VP11/12 abundance and electrophoretic mobility in the presence and absence of US3PK. One million Vero cells were infected with the indicated viruses and lysed at 8 or 12 hpi. Lysates were resolved by 8% SDS-PAGE, transferred to nitrocellulose, and subjected to immunoblot analysis using infrared imaging (top). Detection of all VP11/12 species in KOS-37 and US3-null samples was quantitated and normalized to actin levels (bottom).

4.11 VP11/12 POST-TRANSLATIONAL MODIFICATION

The pronounced abundance of multiple α-VP11/12-reactive species in US3-null infection (Figure 4-11) prompted the examination of what these bands of decreased electrophoretic mobility may have been. As the lab has shown VP11/12 to be highly tyrosine-phosphorylated in certain cell lines (Zahariadis *et al.*, 2008), one hypothesis was that the bands of lesser electrophoretic mobility may represent post-translationally modified VP11/12, specifically singly and multiply tyrosine-phosphorylated VP11/12 species.

One million HeLa cells were subject to the same infection and immunoblotting protocol as described in Section 4-10. Here, however, blots

were further probed for phosphotyrosyl moieties (Figure 4-12); while the blot described in the previous section (Figure 4-11) was probed for phosphotyrosine, none was detected (data not shown). KOS-37 infection at 12 h showed a distinct set of tyrosine-phosphorylated proteins of apparent molecular weight comparable to that of VP11/12. However, overlay of the detected bands of both VP11/12 and phospho-Tyr revealed that their positions on the blot do not correspond. This shows that phospho-Tyr and VP11/12 do not co-migrate, and suggests VP11/12 here is not tyrosine-phosphorylated.

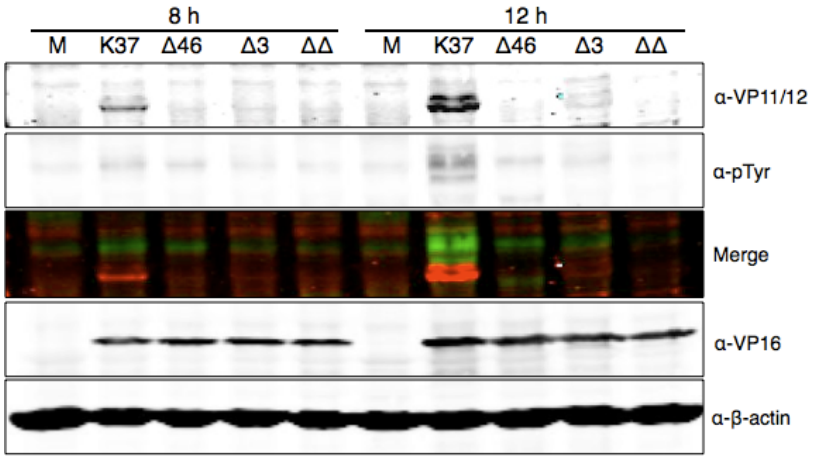

Figure 4-12. VP11/12 electrophoretic mobility shift does not correspond with phosphotyrosine detection. One million HeLa cells were infected with the indicated viruses and lysed at 8 or 12 hpi. Lysates were resolved by 8% SDS-PAGE, transferred to nitrocellulose, and subjected to immunoblot analysis using infrared imaging.

4.12 SUMMARY

US3-null, double knock-out viruses, and their repairs were generated from the parental KOS-37 BACmid. At each intermediate step, screening using PCR allowed verification that the target recombination was occurring.

Mutant viruses generated from these BACmids allow the lab to address questions regarding VP11/12 and US3PK co-dependence. Holly

Saffran confirmed the VP11/12 mobility-shift effect in US3-null infection. Dr. Heather Eaton showed that the double knock-out infection induces greater levels of apoptosis relative to the single US3 knock-out infection. Kevin Quach has investigated whether US3PK phosphorylates Akt targets independent of VP11/12-induced Akt activation.

Chapter V
Discussion

5.1 RESULTS SUMMARY

Several putative SH2 binding motifs are well conserved among VP11/12 orthologues of *Simplexvirus* species, including predicted SFK SH2 binding motif YEEI. A synthetic peptide of VP11/12-derived phospho-YEEI-containing sequence binds directly to Lck SH2, and this phenomenon is phosphorylation- and sequence-dependent. Lck SH2 binds VP11/12, an interaction that can be inhibited in a concentration-dependent manner with pYEEI peptide, suggesting competitive inhibition. This inhibition of the interaction is likewise dependent on peptide sequence and phosphorylation state. In comparing the SH2 reactivity of phospho-YEEI with that of the Lck-endogenous inhibitory phosphomotif, phospho-YEEI shows greater affinity to Lck SH2 than the Lck-derived sequence.

US3PK-deficient mutants were generated via recombineering. Preliminary analysis of these mutants was performed with observations as follows. The enhanced Akt activation observed in a US3-null mutant depends on VP11/12. Apparent VP11/12 expression level is not dependent on US3PK in HSV-1 infection. The posttranslational modification, however, is dependent on US3PK, and this is not phosphotyrosyl modification.

5.2 STRENGTHENING THE WAGNER-SMILEY MODEL

5.2.1 Testing the initiating interaction

The Wagner-Smiley model of VP11/12-induced Akt activation describes how VP11/12, using its phospho-YEEI SH2 binding motif, commandeers SFKs, most notably Lck, to become heavily tyrosine-phosphorylated, completing the phosphomotifs necessary for binding various signalling adaptor molecules. Several implications

necessarily follow from this model and are tested here: (i) VP11/12-derived phospho-YEEI sequence directly binds the Lck SH2 domain; (ii) the canonical SH2 binding mechanism is how (i) occurs; (iii) by virtue of (i) and (ii), and if phospho-YEEI is in fact responsible for Lck activation, then phospho-YEEI has demonstrably greater affinity for the Lck SH2 domain than the Lck inhibitory motif; and (iv) the Lck SH2 domain binds full-length VP11/12. In Chapter 3, the described experiments test these first steps critical to the Wagner-Smiley model.

If phospho-YEEI of VP11/12 is indeed a critical mediator of SFK activation, it follows that the pYEEI peptide binds the Lck SH2 domain and does so directly. Indeed, pYEEI was capable of co-precipitating purified Lck SH2 domain from solution (Figure 3-6).

Should this pYEEI-SH2 interaction occur via the canonical SH2 binding mechanism at its binding cleft as described by Waksman *et al*. (1993), non-phosphorylated and sequence-nonspecific peptide would show less affinity for the Lck SH2 domain. In line with that prediction, sequence-nonspecific peptide shows markedly reduced SH2 affinity and non-phosphorylated YEEI peptide affinity is abrogated relative to pYEEI (Figures 3-6, 3-8, and 3-9).

Given that phospho-YEEI binds the SH2 domain via its canonical binding groove at the same site the Lck inhibitory motif adheres, phospho-YEEI-mediated Lck activation implies the Lck SH2 domain preferentially binds phospho-YEEI over the Lck inhibitory motif. The results cohere with that prediction as the Lck SH2 domain has greater affinity for pYEEI peptide than the inhibitory phosphomotif peptide (Figures 3-6 and 3-11).

The model illustrates that the SH2-VP11/12 interaction is the critical interaction, which implies that the SH2 domain is sufficient for interaction with full-length VP11/12, not just peptide derivatives. The results here

show that SH2, without the remainder of Lck, interacts with full-length VP11/12 (Figure 3-4).

The experiments described in Chapter 3 each test necessary assumptions and implications of the Wagner-Smiley model. None of the observations undermine the model. Considering these results, we can speak with more confidence regarding the model's specifics. VP11/12 uses its phospho-YEEI motif to out-compete the Lck inhibitory motif at the canonical SH2 binding site to prop open Lck, inducing its activation.

5.2.2 Qualifications of support

It is important to acknowledge that the each of the experimental strategies outlined in Chapter 3 is a highly reductionist representation of the *in vivo* environment. The findings here do not necessarily reflect the context of viral infection.

The peptide pull-down assays were performed to demonstrate direct binding and offer some indication of differential SH2 reactivity among peptides (Figure 3-6). Conclusions from this experimental model, however, presume that YEEI is not obscured by protein folding. As the immobilized peptides were synthetic dodecamers, they lacked the secondary and tertiary structure present in full-length proteins that may bury the motif of interest. VP11/12 amino acid sequence (accession no. NP_044648.1) was analyzed with NetSurfP 1.1 (Petersen *et al.*, 2009) for residue surface accessibility, producing a result that underscores this weakness. The accessibility analysis revealed a prediction that Tyr-624 of YEEI is buried; given statistical comparison of the sequence to a large control set of solved structures and corresponding sequences, NetSurfP showed that this was a high-reliability prediction. On the other hand, this nonempirical and purely informatic analysis cannot account for the posttranslational modification of VP11/12 that conceivably alters folding kinetics. In any case, the

conclusions from these peptide pull-down experiments are valid if and only if the motifs are exposed and capable of SH2 interaction in the context of full-length protein.

The predictions of the surface accessibility analysis suggest a further refinement to the Wagner-Smiley model. Though twenty-one of 23 Tyr residues on VP11/12 are predicted to be buried, VP11/12 is known to be heavily tyrosine-phosphorylated in lymphocytes (Zahariadis *et al*., 2008). Surface-accessible serines or threonines may be phosphorylated to elicit conformational changes that expose these tyrosines, allowing tyrosine-phosphorylation. If upon Ser/Thr-phosphorylation these otherwise-buried tyrosine residues are forced into an exposed orientation, VP11/12 is pliable in response to phosphorylation. This is consistent with the idea of VP11/12 acting as a scaffold for various signalling adaptor molecules, extending its docking sites for binding and co-localization of various binding partners. The results of the peptide competition assays offer further insight.

The experimental strategy of GST pull-down with peptide competition was used to further test the SH2 reactivity of each peptide sequence. The observation that phosphotyrosyl peptide competes away SH2-VP11/12 adherence suggests that phosphotyrosyl moieties are surface-accessible and relevant to the interaction.

A peptide competition assay analogous to mine was used by Songyang *et al*. (1993) to first characterize SH2-phosphomotif interaction. These experiments demonstrated that SH2-reactive peptides, in particular pYEEI, are capable of competitively inhibiting SH2-VP11/12 interaction (Figure 3-8). Taken with the evidence that pYEEI binds the SH2 domain at its binding groove (section 3.5), we can conclude that the binding groove is important for SH2-VP11/12 association. It would be overreaching to conclude that phospho-YEEI on VP11/12 is necessary for this interaction,

but it is sufficient. Indeed, more recent observations by the lab have refuted the idea that phospho-YEEI is necessary: a Y624F substitution in VP11/12 does not observably inhibit Lck interaction and only partially inhibits Akt activation (Ulrike Strunk, Holly Saffran, and James Smiley, unpublished data). Accordingly, these observations have led Ulrike Strunk to her current investigation of other tyrosyl elements on VP11/12 for their importance in SFK activation (discussed in subsection 5.2.3).

The peptide competition assays may raise further questions about how VP11/12 binds SH2. Maximal concentrations of pYEEI failed to completely inhibit SH2-VP11/12 binding (Figure 3-8). While there is some evidence here for VP11/12 binding at the canonical SH2 cleft, there is no evidence here to contradict the idea that VP11/12 binds SH2 domains at other sites and that these play a role in VP11/12 recruitment of SFKs.

The support that Chapter 3 offers for the Wagner-Smiley model is contingent on the assumption that the phosphomotifs of VP11/12 are surface accessible. This evidence supports a mechanism but does not preclude other concurrent mechanisms for SH2-VP11/12 interaction.

5.2.3 Further investigation in the lab

These findings must be replicated in an *in vivo* infection model for further indication of the relevance the phosphomotifs. To that end, Holly Saffran and Ulrike Strunk of the lab have generated and are generating KOS-37 virus expressing GFP-tagged VP11/12 with various Tyr-to-Phe substitutions at conserved Tyr residues to abrogate their phorphorylatability, including Y624F in the YEEI motif of interest here. Recent characterization of these mutants thus far has shed light on the importance of YEEI and other motifs.

VP11/12(Y624F) retains the Lck-binding capability of wild-type VP11/12, but its Akt-activatory signalling is notably inhibited (Strunk,

Saffran, and Smiley, unpublished data). This suggests that a mechanism that does not require phospho-YEEI can at least partially activate Lck and produce an intermediate phenotype.

Conservation of several putative phosphotyrosyl binding motifs leads to the hypotheses that each are relevant and functional motifs. Strunk hypothesized that the conserved tyrosine Y613 as part of YETV (Figure 3-1) is another relevant phosphotyrosyl moiety for Lck activation. VP11/12(Y613F) had a phenotype equivalent to VP11/12(Y624F) (Strunk and Smiley, unpublished data). That is, Y613F produced Lck recruitment comparable to and decreased Akt activation relative to wild-type VP11/12. A double mutant (Y624F and Y613F) abrogated the Lck-recruiting and Akt-activatory phenotype (Strunk and Smiley, unpublished data). These data suggest that Y624 and Y613 are functionally redundant, either being sufficient for intermediate wild-type phenotype, both being necessary for full wild-type effects.

These observations also suggest that YETV has SH2 reactivity comparable to YEEI, and considering the established SH2 binding mechanism helps us explain the YETV-YEEI equivalence. Assuming tyrosine-phosphorylation, YEEI was shown to be the optimal- affinity SH2-binding sequence (Songyang *et al.*, 1993), and the structure of the SH2-YEEI complex was solved (Waksman *et al.*, 1993), giving rise to the canonical SH2 binding mechanism. In comparing YEEI and YETV, Tyr and Glu are the same, but two motifs differ at their Y+2 and Y+3 positions.

Waksman *et al.* (1993) describe in detail the interactions that must be acting upon each of the four residues of the binding motif. The Y+2 position interacts at the surface of the SH2 domain and therefore strongly favours hydrophilic residues. The Glu of YEEI fully satisfies this criterion, but Thr of YETV does not. However, given that Strunk has demonstrated YETV equivalence to YEEI, I would hypothesize that Thr-615 is phosphorylated,

and must be phosphorylated for efficient SH2-YETV binding. In congruence with this hypothesis, orthologous *Simplexvirus* VP11/12 residues aligned with T615 (Figure 3-1) are each phosphorylatable or negatively charged, conservation suggesting a functional significance to the charge of this residue. A charged phospho-T would be hydrophilic and would agree with the mechanism supported by Waksman *et al*. (1993). The Y+3 residue interacts at a hydrophobic binding pocket with most of its surface area engulfed by this pocket. The Y+3 of a strongly SH2-reactive binding motif should be hydrophobic. Similar to the Ile of YEEI, the Y+3 valine residue of YETV is also a large, branch-chained, hydrophobic residue, so valine at Y+3 is congruent with the Waksman *et al*. (1993) mechanism. The comparability of YEEI and YETV can be explained if Thr-615 is indeed phosphorylated.

The lab also undertook the mutation of YENV (Grb2 SH2 motif) to FENV to investigate Grb2 SH2 interaction, and NPLY (Shc PTB motif) to NPLF was generated to examine PTB interaction (Figure 3-1; Strunk and Smiley, unpublished data). In line with expectations, the interactions are each inhibited by the respective mutations.

5.2.4 Going forward (and backward)

Future investigation must focus on testing and extending the Wagner-Smiley model forward and backward, after and before the initiating Lck-activatory event. As we look backward, it is unclear what factors lead to the phosphorylation of YEEI. YEEI is not SH2-reactive without phosphorylation, so phosphorylation must be a critical event. VP11/12-dependent SFK activation is cell type-specific (Zahariadis *et al*., 2008), greater in lymphocytes than in Vero cell and fibroblasts. One could presume that such Lck activation is present in each cell type that shows VP11/12-dependent Akt activation, as is the case in HEL fibroblasts (Wagner and Smiley, 2011). A hypothesis is that the kinase responsible for

YEEI phosphorylation is tissue-specific. Looking forward, the relevance of the recruitment of PI3K, Grb2, and Shc should be investigated fully. In particular, whether factors downstream of Shc-Grb2 co-localization are activated in a VP11/12-dependent manner must be examined.

Investigating events downstream of PI3K in viral infection has led to curious findings. As shown by both the lab (Quach and Smiley, unpublished data; Quach, 2013) and Chuluunbaatar *et al*. (2010), while phospho-Akt is readily detectable in HSV-1 infection, phosphorylation of Akt effectors is not dependent on Akt activation, as would be the case in an uninfected context. Quach (2013) found that FBS-induced Akt activation during infection with UL46- and US3-null virus (Chapter 4) does not correspond to phosphorylation of known Akt-downstream targets GSK3β and 4E-BP1 as it does in the mock-infected context. Thus, HSV-1 can block the transduction of signals past Akt, independent of US3PK and VP11/12. Quach (2013) showed that US3PK, not Akt, is responsible for phosphorylation of a select number of Akt effectors during infection, as effector phosphorylation was US3-dependent.

The curious blockade of signalling to Akt effectors from Akt and simultaneous takeover of its signalling node by US3PK remains to be reconciled with the Wagner-Smiley model. That is, the purpose of VP11/12-dependent Akt activation is unclear when we consider viral attenuation of Akt signalling. We cannot rule out the possibility that, while VP11/12 activates Akt, the action of Akt is not wholly blocked but rather redirected.

VP11/12 has also been observed to bind Shc and Grb2 (Strunk, Saffran, and Smiley, unpublished data). Polyoma virus middle T antigen also recruits Shc and Grb2 (reviewed by Cheng *et al*., 2009). In that case, such a complex results in the recruitment of SOS, a guanine nucleotide exchange factor that activates Ras. Whether Wagner-Smiley initiation results in

analogous events can be investigated. Experiments should address whether SOS is co-precipitated with the VP11/12-Shc-Grb2 complex. If so, Ras activation assays are commercially available, functioning on the premise of selective activated-Ras precipitation and immunoblot analysis of Ras levels. We should ask if Ras is activated in a VP11/12-dependent manner by comparing activation levels of wild-type and UL46-null viruses. With the US3-null virus described here, we should also ask if Ras activation is enhanced in response to US3-deletion. Commercially available phospho-specific antibodies for factors downstream of Ras allow for immunoblot analysis of VP11/12-dependent signal transduction from Ras. All things considered, the primary function of VP11/12 may not necessarily be the induction of PI3K-Akt flux, but rather the scaffolding of Grb2 and Shc, and the events thereafter.

5.3 INTERPLAY OF US3PK AND VP11/12

5.3.1 Confounding findings in US3PK characterization

Characterization of US3PK and its influence at various points in Akt signalling has led to findings that are difficult to interpret, not only downstream (as outlined in subsection 5.2.4) but upstream of Akt. In HSV-2 orthologues, Matsuzaki *et al*. (2005) showed that US3PK phosphorylates VP11/12, and that in US3-null infection VP11/12 stability is measurably attenuated. Benetti and Roizman (2006) found that US3PK inhibits Akt activation. Taken together with Wagner and Smiley's (2011) demonstration of VP11/12 importance in Akt activation, it would be strange to find US3PK, itself an inhibitor of Akt, enhancing the expression levels of VP11/12, an Akt activator. UL46- and US3-null double and single mutants were generated (Zahariadis *et al*., 2008; Chapter 4) to help address this oddity.

5.3.2 VP11/12 abundance does not depend on US3PK

While Matsuzaki *et al*. (2005) found that apparent VP11/12 expression is diminished in US3 knock-out HSV-2 infection, my findings (Figure 4-11) in contrast do not support that result in HSV-1 infection. This suggests that HSV-1 VP11/12 and US3PK do not necessarily share the same functional relationship as HSV-2 VP11/12 and US3PK.

The HSV-1 orthologues should be investigated with the same methods that Matsuzaki *et al*. (2005) used in HSV-2 to determine if analogous interaction exists for HSV-1. Matsuzaki *et al*. (2005) performed a pulse-chase assay to examine VP11/12 stability. They pulsed the culture medium with radiolabelled methionine, chased with radiolabel-free medium, and measured radioactivity by exposure to radiation-sensitive film, comparing wild-type to US3-null infection. Matsuzaki *et al*. (2005) also demonstrated that US3PK can directly phosphorylate VP11/12 by *in vitro* kinase assay. Purified US3PK (or kinase-inactivated US3PK) and purified, immobilized VP11/12 were incubated together in a buffer containing radiolabelled ATP. The resultant VP11/12 was assayed for radioactivity. Equivalent stability and kinase assays in the HSV-1 context would help resolve if these two sets of orthologues indeed differ in how VP11/12 interacts with US3PK.

5.3.3 VP11/12 modification is US3PK-dependent

The presence or absence of US3PK has an observable influence on VP11/12 electrophoretic-mobility species (Figure 4-11), possibly due to posttranslational modification that is not tyrosine-phosphorylation (Figure 4-12). Without US3PK (Figure 4-11), VP11/12 species of apparently greater molecular weight are present. The lab recently showed that these hypomobile VP11/12 species are the result of phosphorylation, as phosphatase treatment collapses these species into the band of greatest mobility (Saffran and Smiley, unpublished data).

Anti-phosphotyrosine-reactive bands were shown to co-migrate with the retarded VP11/12 species after infection of HFF cells and were enhanced in US3-null infection (Saffran and Smiley, unpublished data). This suggests tyrosine phosphorylation on VP11/12, which contradicts my finding, and that tyrosine phosphorylation is suppressed by US3PK, but Saffran's result does not address Ser/Thr phosphorylation.

Under the premise that US3PK down-regulates VP11/12 tyrosine phosphorylation, we can test if this has consequences for Wagner-Smiley signalling. Ectopic overexpression of US3PK from an inducible vector should inhibit VP11/12 signalling activity and corresponding recruitment of aforementioned signalling molecules, and greater induction of this vector should inhibit this activity further. If the predicted observations were true, this would support the idea that US3PK inhibits Akt by inhibiting VP11/12 phosphorylation.

US3PK may activate an effector, any number of intermediaries, that modulates VP11/12 modification. Given the promiscuous nature of US3PK, the effect may be due to one or more of many targets. Nevertheless, determining how the presence or absence of US3PK promotes or suppresses VP11/12 modification or function presents an additional avenue for investigation.

A situation where VP11/12 modification may be a relevant variable is virion packaging. Murphy *et al*. (2008) observed VP11/12 phospho-species with VP11/12-overexpression. They showed that extracellular virions, isolated by fractionation in a sucrose gradient, had captured only select VP11/12 mobility species (of many observed) for packaging. Given that US3PK action results in VP11/12 phosphorylation, we should ask whether this modulation of VP11/12 phosphorylation affects which species are preferred for packaging or membrane association. By isolation of extracellular virions as per Murphy *et al*. (2008), immunoblot

analysis of virions comparing VP11/12 species, between US3-null to wild-type infection, should allow us to answer if US3PK changes what VP11/12 phospho-species are preferred for packaging. Where VP11/12 phosphorylation may be relevant for VP11/12 function, the US3 mutants may prove useful for experimentation.

5.4 CLOSING COMMENTS

The investigations presented in this document aimed to illuminate the role of VP11/12 and US3PK in HSV-1-induced cellular signalling. The findings help refine the Wagner-Smiley model of how VP11/12 interacts with its binding partners. The US3/UL46 mutants allow the further exploration of US3-VP11/12 interplay in virus-induced signalling. These issues deserve further consideration.

Bibliography

1. Altschul SF, Koonin EV. Iterated profile searches with PSI-BLAST--a tool for discovery in protein databases. Trends Biochem Sci. 1998 Nov;23(11):444-7.
2. Alwine JC, Steinhart WL, Hill CW. Transcription of herpes simplex type 1 DNA in nuclei isolated from infected HEp-2 and KB cells. Virology. 1974 Jul;60(1):302-7.
3. Amanchy R, Zhong J, Hong R, Kim JH, Gucek M, Cole RN, et al. Identification of c-src tyrosine kinase substrates in platelet-derived growth factor receptor signaling. Mol Oncol. 2009 Dec;3(5-6):439-50.
4. Andjelkovic M, Alessi DR, Meier R, Fernandez A, Lamb NJ, Frech M, et al. Role of translocation in the activation and function of protein kinase B. J Biol Chem. 1997 Dec 12;272(50):31515-24.
5. Auger KR, Serunian LA, Soltoff SP, Libby P, Cantley LC. PDGF-dependent tyrosine phosphorylation stimulates production of novel polyphosphoinositides in intact cells. Cell. 1989 Apr 7;57(1):167-75.
6. Bai X, Ma D, Liu A, Shen X, Wang QJ, Liu Y, et al. Rheb activates mTOR by antagonizing its endogenous inhibitor, FKBP38. Science. 2007 Nov 9;318(5852):977-80.
7. Bellacosa A, Testa JR, Staal SP, Tsichlis PN. A retroviral oncogene, akt, encoding a serine-threonine kinase containing an SH2-like region. Science. 1991 Oct 11;254(5029):274-7.
8. Benetti L, Roizman B. Protein kinase B/Akt is present in activated form throughout the entire replicative cycle of deltaU(S)3 mutant virus but only at early times after infection with wild-type herpes simplex virus 1. J Virol. 2006 Apr;80(7):3341-8.
9. Bromann PA, Korkaya H, Courtneidge SA. The interplay between src family kinases and receptor tyrosine kinases. Oncogene. 2004 Oct

18;23(48):7957-68.
10. Burnham MR, Bruce-Staskal PJ, Harte MT, Weidow CL, Ma A, Weed SA, et al. Regulation of c-SRC activity and function by the adapter protein CAS. Mol Cell Biol. 2000 Aug;20(16):5865-78.
11. Calleja V, Alcor D, Laguerre M, Park J, Vojnovic B, Hemmings BA, et al. Intramolecular and intermolecular interactions of protein kinase B define its activation in vivo. PLoS Biol. 2007 Apr;5(4):e95.
12. Cardone MH, Roy N, Stennicke HR, Salvesen GS, Franke TF, Stanbridge E, et al. Regulation of cell death protease caspase-9 by phosphorylation. Science. 1998 Nov 13;282(5392):1318-21.
13. Cartier A, Broberg E, Komai T, Henriksson M, Masucci MG. The herpes simplex virus-1 Us3 protein kinase blocks CD8T cell lysis by preventing the cleavage of bid by granzyme B. Cell Death Differ. 2003 Dec;10(12):1320-8.
14. Cheng J, DeCaprio JA, Fluck MM, Schaffhausen BS. Cellular transformation by simian virus 40 and murine polyoma virus T antigens. Semin Cancer Biol. 2009 Aug;19(4):218-28.
15. Chuluunbaatar U, Roller R, Feldman ME, Brown S, Shokat KM, Mohr I. Constitutive mTORC1 activation by a herpesvirus akt surrogate stimulates mRNA translation and viral replication. Genes Dev. 2010 Dec 1;24(23):2627-39.
16. Cocchi F, Menotti L, Dubreuil P, Lopez M, Campadelli-Fiume G. Cell-to-cell spread of wild-type herpes simplex virus type 1, but not of syncytial strains, is mediated by the immunoglobulin-like receptors that mediate virion entry, nectin1 (PRR1/HveC/HIgR) and nectin2 (PRR2/HveB). J Virol. 2000 Apr;74(8):3909-17.
17. Cohen JI, Straus SE, Arvin AM. Varicella-zoster virus replication, pathogenesis, and management. In: Knipe DM, Howley PM, editors. Fields Virology. 5th Edition ed. Lippincott Williams & Wilkins; 2007. p. 2774-818.
18. Copeland AM, Newcomb WW, Brown JC. Herpes simplex virus

replication: Roles of viral proteins and nucleoporins in capsid-nucleus attachment. J Virol. 2009 Feb;83(4):1660-8.
19. Copen CE, Chandra A, Martinez G. Prevalence and timing of oral sex with opposite-sex partners among females and males aged 15â€“24 years: United states, 2007â€“2010. National Health Statistics Reports. USA: Centers for Disease Control and Prevention; 2012. Report No.: 56.
20. Cuevas B, Lu Y, Watt S, Kumar R, Zhang J, Siminovitch KA, et al. SHP-1 regulates lck-induced phosphatidylinositol 3-kinase phosphorylation and activity. J Biol Chem. 1999 Sep 24;274(39):27583-9.
21. Danial NN. BAD: Undertaker by night, candyman by day. Oncogene. 2008 Dec;27 Suppl 1:S53-70.
22. Datta SR, Dudek H, Tao X, Masters S, Fu H, Gotoh Y, et al. Akt phosphorylation of BAD couples survival signals to the cell-intrinsic death machinery. Cell. 1997 Oct 17;91(2):231-41.
23. Davison AJ, Eberle R, Ehlers B, Hayward GS, McGeoch DJ, Minson AC, et al. The order herpesvirales. Arch Virol. 2009;154(1):171-7.
24. DeLuca NA, McCarthy AM, Schaffer PA. Isolation and characterization of deletion mutants of herpes simplex virus type 1 in the gene encoding immediate-early regulatory protein ICP4. J Virol. 1985 Nov;56(2):558-70.
25. Deshmane SL, Fraser NW. During latency, herpes simplex virus type 1 DNA is associated with nucleosomes in a chromatin structure. J Virol. 1989 Feb;63(2):943-7.
26. Diefenbach RJ, Miranda-Saksena M, Douglas MW, Cunningham AL. Transport and egress of herpes simplex virus in neurons. Rev Med Virol. 2008 Jan-Feb;18(1):35-51.
27. Dohner K, Wolfstein A, Prank U, Echeverri C, Dujardin D, Vallee R, et al. Function of dynein and dynactin in herpes simplex virus capsid transport. Mol Biol Cell. 2002 Aug;13(8):2795-809.
28. Downes CP, Bennett D, McConnachie G, Leslie NR, Pass I, MacPhee C, et

al. Antagonism of PI 3-kinase-dependent signalling pathways by the tumour suppressor protein, PTEN. Biochem Soc Trans. 2001 Nov;29(Pt 6):846-51.
29. Dunant NM, Senften M, Ballmer-Hofer K. Polyomavirus middle-T antigen associates with the kinase domain of src-related tyrosine kinases. J Virol. 1996 Mar;70(3):1323-30.
30. Edwards S, Carne C. Oral sex and the transmission of viral STIs. Sex Transm Infect. 1998 Feb;74(1):6-10.
31. Engelberg R, Carrell D, Krantz E, Corey L, Wald A. Natural history of genital herpes simplex virus type 1 infection. Sex Transm Dis. 2003 Feb;30(2):174-7.
32. Facchinetti V, Ouyang W, Wei H, Soto N, Lazorchak A, Gould C, et al. The mammalian target of rapamycin complex 2 controls folding and stability of akt and protein kinase C. EMBO J. 2008 Jul 23;27(14):1932-43.
33. Fantl WJ, Johnson DE, Williams LT. Signalling by receptor tyrosine kinases. Annu Rev Biochem. 1993;62:453-81.
34. Farnsworth A, Wisner TW, Webb M, Roller R, Cohen G, Eisenberg R, et al. Herpes simplex virus glycoproteins gB and gH function in fusion between the virion envelope and the outer nuclear membrane. Proc Natl Acad Sci U S A. 2007 Jun 12;104(24):10187-92.
35. Ganem D. Kaposi's sarcoma-associated herpesvirus. In: Knipe DM, Howley PM, editors. Fields Virology. 5th Edition ed. Lippincott Williams & Wilkins; 2007. p. 2847-88.
36. Gao X, Pan D. TSC1 and TSC2 tumor suppressors antagonize insulin signaling in cell growth. Genes Dev. 2001 Jun 1;15(11):1383-92.
37. Garber DA, Schaffer PA, Knipe DM. A LAT-associated function reduces productive-cycle gene expression during acute infection of murine sensory neurons with herpes simplex virus type 1. J Virol. 1997 Aug;71(8):5885-93.
38. Gierasch WW, Zimmerman DL, Ward SL, Vanheyningen TK, Romine JD, Leib DA. Construction and characterization of bacterial artificial

chromosomes containing HSV-1 strains 17 and KOS. J Virol Methods. 2006 Aug;135(2):197-206.
39. Goldsmith MA, Weiss A. Isolation and characterization of a T-lymphocyte somatic mutant with altered signal transduction by the antigen receptor. Proc Natl Acad Sci U S A. 1987 Oct;84(19):6879-83.
40. Granzow H, Klupp BG, Mettenleiter TC. Entry of pseudorabies virus: An immunogold-labeling study. J Virol. 2005 Mar;79(5):3200-5.
41. Hagmann M, Georgiev O, Schaffner W, Douville P. Transcription factors interacting with herpes simplex virus alpha gene promoters in sensory neurons. Nucleic Acids Res. 1995 Dec 25;23(24):4978-85.
42. Hahn-Windgassen A, Nogueira V, Chen CC, Skeen JE, Sonenberg N, Hay N. Akt activates the mammalian target of rapamycin by regulating cellular ATP level and AMPK activity. J Biol Chem. 2005 Sep 16;280(37):32081-9.
43. Hale BG, Jackson D, Chen YH, Lamb RA, Randall RE. Influenza A virus NS1 protein binds p85beta and activates phosphatidylinositol-3-kinase signaling. Proc Natl Acad Sci U S A. 2006 Sep 19;103(38):14194-9.
44. Harper JW, Adami GR, Wei N, Keyomarsi K, Elledge SJ. The p21 cdk-interacting protein Cip1 is a potent inhibitor of G1 cyclin-dependent kinases. Cell. 1993 Nov 19;75(4):805-16.
45. Held K, Derfuss T. Control of HSV-1 latency in human trigeminal ganglia-current overview. J Neurovirol. 2011 Dec;17(6):518-27.
46. Henderson G, Peng W, Jin L, Perng GC, Nesburn AB, Wechsler SL, et al. Regulation of caspase 8- and caspase 9-induced apoptosis by the herpes simplex virus type 1 latency-associated transcript. J Neurovirol. 2002 Dec;8 Suppl 2:103-11.
47. Honess RW, Roizman B. Regulation of herpesvirus macromolecular synthesis: Sequential transition of polypeptide synthesis requires functional viral polypeptides. Proc Natl Acad Sci U S A. 1975 Apr;72(4):1276-80.
48. Howard M, Sellors JW, Jang D, Robinson NJ, Fearon M, Kaczorowski J, et

al. Regional distribution of antibodies to herpes simplex virus type 1 (HSV-1) and HSV-2 in men and women in Ontario, Canada. J Clin Microbiol. 2003 Jan;41(1):84-9.
49. Huang J, Lazear HM, Friedman HM. Completely assembled virus particles detected by transmission electron microscopy in proximal and mid-axons of neurons infected with herpes simplex virus type 1, herpes simplex virus type 2 and pseudorabies virus. Virology. 2011 Jan 5;409(1):12-6.
50. Inoue H, Motani-Saitoh H, Sakurada K, Ikegaya H, Yajima D, Hayakawa M, et al. Detection of varicella-zoster virus DNA in 414 human trigeminal ganglia from cadavers by the polymerase chain reaction: A comparison of the detection rate of varicella-zoster virus and herpes simplex virus type 1. J Med Virol. 2010 Feb;82(2):345-9.
51. Kato A, Yamamoto M, Ohno T, Tanaka M, Sata T, Nishiyama Y, et al. Herpes simplex virus 1-encoded protein kinase UL13 phosphorylates viral Us3 protein kinase and regulates nuclear localization of viral envelopment factors UL34 and UL31. J Virol. 2006 Feb;80(3):1476-86.
52. Kato K, Daikoku T, Goshima F, Kume H, Yamaki K, Nishiyama Y. Synthesis, subcellular localization and VP16 interaction of the herpes simplex virus type 2 UL46 gene product. Arch Virol. 2000;145(10):2149-62.
53. Katoh K, Misawa K, Kuma K, Miyata T. MAFFT: A novel method for rapid multiple sequence alignment based on fast fourier transform. Nucleic Acids Res. 2002 Jul 15;30(14):3059-66.
54. Koegl M, Zlatkine P, Ley SC, Courtneidge SA, Magee AI. Palmitoylation of multiple src-family kinases at a homologous N-terminal motif. Biochem J. 1994 Nov 1;303 (Pt 3)(Pt 3):749-53.
55. Krause PR, Croen KD, Straus SE, Ostrove JM. Detection and preliminary characterization of herpes simplex virus type 1 transcripts in latently infected human trigeminal ganglia. J Virol. 1988 Dec;62(12):4819-23.
56. Kubat NJ, Tran RK, McAnany P, Bloom DC. Specific histone tail

modification and not DNA methylation is a determinant of herpes simplex virus type 1 latent gene expression. J Virol. 2004 Feb;78(3):1139-49.
57. Kuriyan J, Cowburn D. Modular peptide recognition domains in eukaryotic signaling. Annu Rev Biophys Biomol Struct. 1997;26:259-88.
58. Lafferty WE, Downey L, Celum C, Wald A. Herpes simplex virus type 1 as a cause of genital herpes: Impact on surveillance and prevention. J Infect Dis. 2000 Apr;181(4):1454-7.
59. Lau C, Wang X, Song L, North M, Wiehler S, Proud D, et al. Syk associates with clathrin and mediates phosphatidylinositol 3-kinase activation during human rhinovirus internalization. J Immunol. 2008 Jan 15;180(2):870-80.
60. Lei H, Furlong PJ, Ra JH, Mullins D, Cantor R, Fraker DL, et al. AKT activation and response to interferon-beta in human cancer cells. Cancer Biol Ther. 2005 Jul;4(7):709-15.
61. Leopardi R, Van Sant C, Roizman B. The herpes simplex virus 1 protein kinase US3 is required for protection from apoptosis induced by the virus. Proc Natl Acad Sci U S A. 1997 Jul 22;94(15):7891-6.
62. Liang Y, Roizman B. State and role of SRC family kinases in replication of herpes simplex virus 1. J Virol. 2006 Apr;80(7):3349-59.
63. Liedtke W, Opalka B, Zimmermann CW, Lignitz E. Age distribution of latent herpes simplex virus 1 and varicella-zoster virus genome in human nervous tissue. J Neurol Sci. 1993 May;116(1):6-11.
64. Lillycrop KA, Dent CL, Wheatley SC, Beech MN, Ninkina NN, Wood JN, et al. The octamer-binding protein oct-2 represses HSV immediate-early genes in cell lines derived from latently infectable sensory neurons. Neuron. 1991 Sep;7(3):381-90.
65. Liu T, Khanna KM, Chen X, Fink DJ, Hendricks RL. CD8(+) T cells can block herpes simplex virus type 1 (HSV-1) reactivation from latency in sensory neurons. J Exp Med. 2000 May 1;191(9):1459-66.
66. Liu TC, Wakimoto H, Martuza RL, Rabkin SD. Herpes simplex virus Us3(-)

mutant as oncolytic strategy and synergizes with phosphatidylinositol 3-kinase-akt targeting molecular therapeutics. Clin Cancer Res. 2007 Oct 1;13(19):5897-902.
67. Lokshin A, Mayotte JE, Levitt ML. Mechanism of interferon beta-induced squamous differentiation and programmed cell death in human non-small-cell lung cancer cell lines. J Natl Cancer Inst. 1995 Feb 1;87(3):206-12.
68. Maehama T, Dixon JE. The tumor suppressor, PTEN/MMAC1, dephosphorylates the lipid second messenger, phosphatidylinositol 3,4,5-trisphosphate. J Biol Chem. 1998 May 29;273(22):13375-8.
69. Manning BD, Tee AR, Logsdon MN, Blenis J, Cantley LC. Identification of the tuberous sclerosis complex-2 tumor suppressor gene product tuberin as a target of the phosphoinositide 3-kinase/akt pathway. Mol Cell. 2002 Jul;10(1):151-62.
70. Matsuzaki A, Yamauchi Y, Kato A, Goshima F, Kawaguchi Y, Yoshikawa T, et al. US3 protein kinase of herpes simplex virus type 2 is required for the stability of the UL46-encoded tegument protein and its association with virus particles. J Gen Virol. 2005 Jul;86(Pt 7):1979-85.
71. McGeoch DJ, Rixon FJ, Davison AJ. Topics in herpesvirus genomics and evolution. Virus Res. 2006 Apr;117(1):90-104.
72. McKnight JL, Pellett PE, Jenkins FJ, Roizman B. Characterization and nucleotide sequence of two herpes simplex virus 1 genes whose products modulate alpha-trans-inducing factor-dependent activation of alpha genes. J Virol. 1987 Apr;61(4):992-1001.
73. Miller CS, Danaher RJ. Asymptomatic shedding of herpes simplex virus (HSV) in the oral cavity. Oral Surg Oral Med Oral Pathol Oral Radiol Endod. 2008 Jan;105(1):43-50.
74. Minaker RL, Mossman KL, Smiley JR. Functional inaccessibility of quiescent herpes simplex virus genomes. Virol J. 2005 Nov 21;2:85.

75. Mocarski ES, Shenk T, Pass RF. Cytomegaloviruses. In: Knipe DM, Howley PM, editors. Fields Virology. 5th Edition ed. Lippincott Williams & Wilkins; 2007. p. 2702-72.
76. Montgomery RI, Warner MS, Lum BJ, Spear PG. Herpes simplex virus-1 entry into cells mediated by a novel member of the TNF/NGF receptor family. Cell. 1996 Nov 1;87(3):427-36.
77. Moorman NJ, Cristea IM, Terhune SS, Rout MP, Chait BT, Shenk T. Human cytomegalovirus protein UL38 inhibits host cell stress responses by antagonizing the tuberous sclerosis protein complex. Cell Host Microbe. 2008 Apr 17;3(4):253-62.
78. Mou F, Wills E, Baines JD. Phosphorylation of the U(L)31 protein of herpes simplex virus 1 by the U(S)3-encoded kinase regulates localization of the nuclear envelopment complex and egress of nucleocapsids. J Virol. 2009 May;83(10):5181-91.
79. Munger J, Chee AV, Roizman B. The U(S)3 protein kinase blocks apoptosis induced by the d120 mutant of herpes simplex virus 1 at a premitochondrial stage. J Virol. 2001 Jun;75(12):5491-7.
80. Munger J, Roizman B. The US3 protein kinase of herpes simplex virus 1 mediates the posttranslational modification of BAD and prevents BAD-induced programmed cell death in the absence of other viral proteins. Proc Natl Acad Sci U S A. 2001 Aug 28;98(18):10410-5.
81. Murphy MA, Bucks MA, O'Regan KJ, Courtney RJ. The HSV-1 tegument protein pUL46 associates with cellular membranes and viral capsids. Virology. 2008 Jul 5;376(2):279-89.
82. Nada S, Okada M, MacAuley A, Cooper JA, Nakagawa H. Cloning of a complementary DNA for a protein-tyrosine kinase that specifically phosphorylates a negative regulatory site of p60c-src. Nature. 1991 May 2;351(6321):69-72.
83. Nahmias AJ, Lee FK, Beckman-Nahmias S. Sero-epidemiological and

-sociological patterns of herpes simplex virus infection in the world. Scand J Infect Dis Suppl. 1990;69:19-36.
84. Neumann DM, Bhattacharjee PS, Giordani NV, Bloom DC, Hill JM. In vivo changes in the patterns of chromatin structure associated with the latent herpes simplex virus type 1 genome in mouse trigeminal ganglia can be detected at early times after butyrate treatment. J Virol. 2007 Dec;81(23):13248-53.
85. Nilsen A, Myrmel H. Changing trends in genital herpes simplex virus infection in Bergen, Norway. Acta Obstet Gynecol Scand. 2000 Aug;79(8):693-6.
86. Nozawa N, Yamauchi Y, Ohtsuka K, Kawaguchi Y, Nishiyama Y. Formation of aggresome-like structures in herpes simplex virus type 2-infected cells and a potential role in virus assembly. Exp Cell Res. 2004 Oct 1;299(2):486-97.
87. Obenauer JC, Cantley LC, Yaffe MB. Scansite 2.0: Proteome-wide prediction of cell signaling interactions using short sequence motifs. Nucleic Acids Res. 2003 Jul 1;31(13):3635-41.
88. Ostergaard HL, Shackelford DA, Hurley TR, Johnson P, Hyman R, Sefton BM, et al. Expression of CD45 alters phosphorylation of the lck-encoded tyrosine protein kinase in murine lymphoma T-cell lines. Proc Natl Acad Sci U S A. 1989 Nov;86(22):8959-63.
89. Ottensmeyer FP, Beniac DR, Luo RZ, Yip CC. Mechanism of transmembrane signaling: Insulin binding and the insulin receptor. Biochemistry. 2000 Oct 10;39(40):12103-12.
90. Park R, Baines JD. Herpes simplex virus type 1 infection induces activation and recruitment of protein kinase C to the nuclear membrane and increased phosphorylation of lamin B. J Virol. 2006 Jan;80(1):494-504.
91. Pawson T, Nash P. Protein-protein interactions define specificity in signal transduction. Genes Dev. 2000 May 1;14(9):1027-47.

92. Pawson T, Scott JD. Signaling through scaffold, anchoring, and adaptor proteins. Science. 1997 Dec 19;278(5346):2075-80.
93. Pellett PE, Roizman B. The family herpesviridae: A brief introduction. In: Knipe DM, Howley PM, editors. Fields Virology. 5th Edition ed. Lippincott Williams & Wilkins; 2007. p. 2479-99.
94. Peng L, Liang D, Tong W, Li J, Yuan Z. Hepatitis C virus NS5A activates the mammalian target of rapamycin (mTOR) pathway, contributing to cell survival by disrupting the interaction between FK506-binding protein 38 (FKBP38) and mTOR. J Biol Chem. 2010 Jul 2;285(27):20870-81.
95. Peri P, Mattila RK, Kantola H, Broberg E, Karttunen HS, Waris M, et al. Herpes simplex virus type 1 Us3 gene deletion influences toll-like receptor responses in cultured monocytic cells. Virol J. 2008 Nov 21;5:140,422X-5-140.
96. Petersen B, Petersen TN, Andersen P, Nielsen M, Lundegaard C. A generic method for assignment of reliability scores applied to solvent accessibility predictions. BMC Struct Biol. 2009 Jul 31;9:51,6807-9-51.
97. Puntervoll P, Linding R, Gemund C, Chabanis-Davidson S, Mattingsdal M, Cameron S, et al. ELM server: A new resource for investigating short functional sites in modular eukaryotic proteins. Nucleic Acids Res. 2003 Jul 1;31(13):3625-30.
98. Purves FC, Longnecker RM, Leader DP, Roizman B. Herpes simplex virus 1 protein kinase is encoded by open reading frame US3 which is not essential for virus growth in cell culture. J Virol. 1987 Sep;61(9):2896-901.
99. Purves FC, Spector D, Roizman B. UL34, the target of the herpes simplex virus U(S)3 protein kinase, is a membrane protein which in its unphosphorylated state associates with novel phosphoproteins. J Virol. 1992 Jul;66(7):4295-303.
100. Purves FC, Spector D, Roizman B. The herpes simplex virus 1 protein kinase encoded by the US3 gene mediates posttranslational modification of

the phosphoprotein encoded by the UL34 gene. J Virol. 1991 Nov;65(11):5757-64.
101. Quach K. HSV-1 remodels PI3-kinase/AKT signaling [dissertation]. Canada: University of Alberta; 2013.
102. Ray CG, Ryan KJ. Herpesviruses. In: Ryan CG, Ryan KJ, editors. Sherris Medical Microbiology. 5th ed. New York: McGraw-Hill; 2010.
103. Reed JC. Bcl-2 family proteins. Oncogene. 1998 Dec 24;17(25):3225-36.
104. Resh MD. Fatty acylation of proteins: New insights into membrane targeting of myristoylated and palmitoylated proteins. Biochim Biophys Acta. 1999 Aug 12;1451(1):1-16.
105. Reynolds AE, Liang L, Baines JD. Conformational changes in the nuclear lamina induced by herpes simplex virus type 1 require genes U(L)31 and U(L)34. J Virol. 2004 Jun;78(11):5564-75.
106. Reynolds AE, Wills EG, Roller RJ, Ryckman BJ, Baines JD. Ultrastructural localization of the herpes simplex virus type 1 UL31, UL34, and US3 proteins suggests specific roles in primary envelopment and egress of nucleocapsids. J Virol. 2002 Sep;76(17):8939-52.
107. Rickinson AB, Kieff E. Epstein-barr virus. In: Knipe DM, Howley PM, editors. Fields Virology. 5th Edition ed. Lippincott Williams & Wilkins; 2007. p. 2656-700.
108. Roberts CM, Pfister JR, Spear SJ. Increasing proportion of herpes simplex virus type 1 as a cause of genital herpes infection in college students. Sex Transm Dis. 2003 Oct;30(10):797-800.
109. Rock DL, Nesburn AB, Ghiasi H, Ong J, Lewis TL, Lokensgard JR, et al. Detection of latency-related viral RNAs in trigeminal ganglia of rabbits latently infected with herpes simplex virus type 1. J Virol. 1987 Dec;61(12):3820-6.
110. Roizman B, Knipe DM, Whitley RJ. Herpes simplex viruses. In: Knipe DM, Howley PM, editors. Fields Virology. 5th Edition ed. Lippincott Williams

& Wilkins; 2007. p. 2502-601.
111. Rossig L, Jadidi AS, Urbich C, Badorff C, Zeiher AM, Dimmeler S. Akt-dependent phosphorylation of p21(Cip1) regulates PCNA binding and proliferation of endothelial cells. Mol Cell Biol. 2001 Aug;21(16):5644-57.
112. Ruvinsky I, Meyuhas O. Ribosomal protein S6 phosphorylation: From protein synthesis to cell size. Trends Biochem Sci. 2006 Jun;31(6):342-8.
113. Sawtell NM. The probability of in vivo reactivation of herpes simplex virus type 1 increases with the number of latently infected neurons in the ganglia. J Virol. 1998 Aug;72(8):6888-92.
114. Sawtell NM, Poon DK, Tansky CS, Thompson RL. The latent herpes simplex virus type 1 genome copy number in individual neurons is virus strain specific and correlates with reactivation. J Virol. 1998 Jul;72(7):5343-50.
115. Sawtell NM, Thompson RL. Rapid in vivo reactivation of herpes simplex virus in latently infected murine ganglionic neurons after transient hyperthermia. J Virol. 1992 Apr;66(4):2150-6.
116. Segal AL, Katcher AH, Brightman VJ, Miller MF. Recurrent herpes labialis, recurrent aphthous ulcers, and the menstrual cycle. J Dent Res. 1974 Jul-Aug;53(4):797-803.
117. Ship II, Miller MF, Ram C. A retrospective study of recurrent herpes labialis (RHL) in a professional population, 1958-1971. Oral Surg Oral Med Oral Pathol. 1977 Nov;44(5):723-30.
118. Shukla D, Liu J, Blaiklock P, Shworak NW, Bai X, Esko JD, et al. A novel role for 3-O-sulfated heparan sulfate in herpes simplex virus 1 entry. Cell. 1999 Oct 1;99(1):13-22.
119. Sicheri F, Kuriyan J. Structures of src-family tyrosine kinases. Curr Opin Struct Biol. 1997 Dec;7(6):777-85.
120. Sicheri F, Moarefi I, Kuriyan J. Crystal structure of the src family tyrosine kinase hck. Nature. 1997 Feb 13;385(6617):602-9.

121. Simmons A, Tscharke DC. Anti-CD8 impairs clearance of herpes simplex virus from the nervous system: Implications for the fate of virally infected neurons. J Exp Med. 1992 May 1;175(5):1337-44.
122. Smith JS, Robinson NJ. Age-specific prevalence of infection with herpes simplex virus types 2 and 1: A global review. J Infect Dis. 2002 Oct 15;186 Suppl 1:S3-28.
123. Songyang Z, Shoelson SE, Chaudhuri M, Gish G, Pawson T, Haser WG, et al. SH2 domains recognize specific phosphopeptide sequences. Cell. 1993 Mar 12;72(5):767-78.
124. Spruance SL, Freeman DJ, Stewart JC, McKeough MB, Wenerstrom LG, Krueger GG, et al. The natural history of ultraviolet radiation-induced herpes simplex labialis and response to therapy with peroral and topical formulations of acyclovir. J Infect Dis. 1991 Apr;163(4):728-34.
125. Stackpole CW. Herpes-type virus of the frog renal adenocarcinoma. I. virus development in tumor transplants maintained at low temperature. J Virol. 1969 Jul;4(1):75-93.
126. Stehelin D, Varmus HE, Bishop JM, Vogt PK. DNA related to the transforming gene(s) of avian sarcoma viruses is present in normal avian DNA. Nature. 1976 Mar 11;260(5547):170-3.
127. Thomas JW, Ellis B, Boerner RJ, Knight WB, White GC,2nd, Schaller MD. SH2- and SH3-mediated interactions between focal adhesion kinase and src. J Biol Chem. 1998 Jan 2;273(1):577-83.
128. Thompson RL, Preston CM, Sawtell NM. De novo synthesis of VP16 coordinates the exit from HSV latency in vivo. PLoS Pathog. 2009 Mar;5(3):e1000352.
129. Thompson RL, Sawtell NM. Replication of herpes simplex virus type 1 within trigeminal ganglia is required for high frequency but not high viral genome copy number latency. J Virol. 2000 Jan;74(2):965-74.
130. Toma HS, Murina AT, Areaux RG,Jr, Neumann DM, Bhattacharjee PS,

Foster TP, et al. Ocular HSV-1 latency, reactivation and recurrent disease. Semin Ophthalmol. 2008 Jul-Aug;23(4):249-73.
131. Turner A, Bruun B, Minson T, Browne H. Glycoproteins gB, gD, and gHgL of herpes simplex virus type 1 are necessary and sufficient to mediate membrane fusion in a cos cell transfection system. J Virol. 1998 Jan;72(1):873-5.
132. Veillette A, Caron L, Fournel M, Pawson T. Regulation of the enzymatic function of the lymphocyte-specific tyrosine protein kinase p56lck by the non-catalytic SH2 and SH3 domains. Oncogene. 1992 May;7(5):971-80.
133. Veillette A, Fournel M. The CD4 associated tyrosine protein kinase p56lck is positively regulated through its site of autophosphorylation. Oncogene. 1990 Oct;5(10):1455-62.
134. Vogt PK, Hart JR, Gymnopoulos M, Jiang H, Kang S, Bader AG, et al. Phosphatidylinositol 3-kinase: The oncoprotein. Curr Top Microbiol Immunol. 2010;347:79-104.
135. von Willebrand M, Baier G, Couture C, Burn P, Mustelin T. Activation of phosphatidylinositol-3-kinase in jurkat T cells depends on the presence of the p56lck tyrosine kinase. Eur J Immunol. 1994 Jan;24(1):234-8.
136. Wagner MJ, Smiley JR. Herpes simplex virus requires VP11/12 to activate src family kinase-phosphoinositide 3-kinase-akt signaling. J Virol. 2011 Mar;85(6):2803-12.
137. Wagner MJ, Smiley JR. Herpes simplex virus requires VP11/12 to induce phosphorylation of the activation loop tyrosine (Y394) of the src family kinase lck in T lymphocytes. J Virol. 2009 Dec;83(23):12452-61.
138. Waksman G, Shoelson SE, Pant N, Cowburn D, Kuriyan J. Binding of a high affinity phosphotyrosyl peptide to the src SH2 domain: Crystal structures of the complexed and peptide-free forms. Cell. 1993 Mar 12;72(5):779-90.
139. Walters MS, Kinchington PR, Banfield BW, Silverstein S.

Hyperphosphorylation of histone deacetylase 2 by alphaherpesvirus US3 kinases. J Virol. 2010 Oct;84(19):9666-76.
140. Wang G, Barrett JW, Stanford M, Werden SJ, Johnston JB, Gao X, et al. Infection of human cancer cells with myxoma virus requires akt activation via interaction with a viral ankyrin-repeat host range factor. Proc Natl Acad Sci U S A. 2006 Mar 21;103(12):4640-5.
141. Wang QY, Zhou C, Johnson KE, Colgrove RC, Coen DM, Knipe DM. Herpesviral latency-associated transcript gene promotes assembly of heterochromatin on viral lytic-gene promoters in latent infection. Proc Natl Acad Sci U S A. 2005 Nov 1;102(44):16055-9.
142. Warming S, Costantino N, Court DL, Jenkins NA, Copeland NG. Simple and highly efficient BAC recombineering using galK selection. Nucleic Acids Res. 2005 Feb 24;33(4):e36.
143. Waterhouse AM, Procter JB, Martin DM, Clamp M, Barton GJ. Jalview version 2--a multiple sequence alignment editor and analysis workbench. Bioinformatics. 2009 May 1;25(9):1189-91.
144. Watson RJ, Clements JB. Characterization of transcription-deficient temperature-sensitive mutants of herpes simplex virus type 1. Virology. 1978 Dec;91(2):364-79.
145. Whitley RJ, Gnann JW. Viral encephalitis: Familiar infections and emerging pathogens. Lancet. 2002 Feb 9;359(9305):507-13.
146. Willard M. Rapid directional translocations in virus replication. J Virol. 2002 May;76(10):5220-32.
147. Williams JC, Weijland A, Gonfloni S, Thompson A, Courtneidge SA, Superti-Furga G, et al. The 2.35 A crystal structure of the inactivated form of chicken src: A dynamic molecule with multiple regulatory interactions. J Mol Biol. 1997 Dec 19;274(5):757-75.
148. Wisner TW, Wright CC, Kato A, Kawaguchi Y, Mou F, Baines JD, et al. Herpesvirus gB-induced fusion between the virion envelope and outer

nuclear membrane during virus egress is regulated by the viral US3 kinase. J Virol. 2009 Apr;83(7):3115-26.
149. Wullschleger S, Loewith R, Hall MN. TOR signaling in growth and metabolism. Cell. 2006 Feb 10;124(3):471-84.
150. Wysocka J, Herr W. The herpes simplex virus VP16-induced complex: The makings of a regulatory switch. Trends Biochem Sci. 2003 Jun;28(6):294-304.
151. Xu W, Harrison SC, Eck MJ. Three-dimensional structure of the tyrosine kinase c-src. Nature. 1997 Feb 13;385(6617):595-602.
152. Yamanishi K, Mori Y, Pellett PE. Human herpesviruses 6 and 7. In: Knipe DM, Howley PM, editors. Fields Virology. 5th Edition ed. Lippincott Williams & Wilkins; 2007. p. 2819-45.
153. Zahariadis G, Wagner MJ, Doepker RC, Maciejko JM, Crider CM, Jerome KR, et al. Cell-type-specific tyrosine phosphorylation of the herpes simplex virus tegument protein VP11/12 encoded by gene UL46. J Virol. 2008 Jul;82(13):6098-108.
154. Zhang Y, Sirko DA, McKnight JL. Role of herpes simplex virus type 1 UL46 and UL47 in alpha TIF-mediated transcriptional induction: Characterization of three viral deletion mutants. J Virol. 1991 Feb;65(2):829-41.